PRINTED CIRCUIT BOARD INTEGRATED ELECTROSTATICALLY ACTUATED MICRO PNEUMATIC VALVE

by

Clinton F. Holtey

A thesis submitted to the faculty of
The University of Utah
in partial fulfillment of the requirements for the degree of

Master of Science

Department of Mechanical Engineering

The University of Utah

December 2009

THE UNIVERSITY OF UTAH GRADUATE SCHOOL

SUPERVISORY COMMITTEE APPROVAL

of a thesis submitted by

Clinton F. Holtey

This thesis has been read by each member of the following supervisory committee and by majority vote has been found to be satisfactory.

Dan Adams

10 Dec 2001

THE UNIVERSITY OF UTAH GRADUATE SCHOOL

FINAL READING APPROVAL

To the Graduate Council of the University of Utah:

I have read the thesis of Clinton F. Holtey in its final form and have found that (1) its format, citations, and bibliographic style are consistent and acceptable; (2) its illustrative materials including figures, tables, and charts are in place; and (3) the final manuscript is satisfactory to the supervisory committee and is ready for submission to The Graduate School.

Date

Bruce K. Gale
Chair: Supervisory Committee

Approved for the Major Department

Timothy A. Ameel
Chair/Dean

Approved for the Graduate Council

Charles A.
Dean of The Graduate School

ABSTRACT

Microfluidics is an emerging field with the potential to develop small, portable lab-on-a-chip equipment. To accomplish this goal of miniaturization, bulky tubes, pumps and valves common to current microfluidic devices must be replaced with micromachined fluid channels with integrated fluid control systems. Pneumatically actuated fluid control devices have been utilized in miniaturizing fluid control, but control of the pneumatics themselves is often a macroscopic process that limits decreasing overall system size. To provide a means for miniaturizing the pneumatics, an electrostatically actuated gas valve was integrated into a printed circuit board (PCB) and constructed utilizing PCB as a substrate for pneumatic channels, the valve structure, and a distribution system. Although electrostatically-actuated, microscale pneumatic valves have been realized previously, the novel PCB integration of pneumatic channels and an electrostatic valve, as presented in this work, allows for rapid prototype construction and electrical circuit integration, which makes the whole system inexpensive and thus possibly disposable. The valve was specifically manufactured by using a copper foil strip as the valve stopper and PCB traces were used as electrodes to generate an electric field to actuate the foil valve stopper over a hole in the PCB substrate, creating a one way valve. The valve could be stacked in multiple layers to create a three-way valve. The valve was tested to have a maximum operational pressure of 17 kPa when operated at 488 V. The valve was found to hold a static pressure of 197 kPa before valve wall rupture.

The maximum life cycle of the valve prototype was found to be approximately 50,000 cycles. A power consumption of 2.2 mW when operated at a frequency of 2 Hz was observed.

TABLE OF CONTENTS

LIST OF FIGURES

LIST OF TABLES

ACKNOWLEDGMENTS

I would like to thank Idaho Technologies for funding the research for this project and the encouragement to expand my horizon by reaching for a unique solution to a daunting challenge. My advisor and mentor, Dr. Bruce Gale, is acknowledged for his time, guidance and patience while guiding the direction of the research. Srinivas Merugu was absolutely indispensible for his help and knowledge of circuits and LAB VIEW to allow a cycle test to be run and data collection, thank you. I would like to thank Adam Nelson for his help in the research and initial prototype trials. Adam's help with that work formed a basis from which a working prototype was eventually created. Finally, I would like to thank my wife, Jessica, for her patience and understanding of the many hours needed to perform this research. Friends and family members offered encouragement.

CHAPTER 1

INTRODUCTION

Background

Microfluidic systems are playing an increasingly important role in the biomedical field, especially for point-of-care DNA analysis and portable pathogen detection devices.[1-3] DNA analysis in a microfluidic system requires precise fluid movement and control. Working with biofluids tends to be a complex operation requiring many tubes, mixers, valves, and pumps. Miniaturization of the entire system, including pumps and valves, into integrated lab-on-chip components, would allow for quick transfer of fluids, and a self-contained system with increased portability and decreased power consumption. Fully integrated biochips have been realized by others including, Hui Liu et al. in 2004.[2] These researchers have successfully integrated the fluid control systems into the fluid transfer and processing chip by means of thermopneumatic pumps and phase change based valves. There, is however, much work to be done in integrating the fluid control devices. Various ways to integrate the fluid control devices exist, and the means by which those devices are actuated contribute to how well it is integrated.

Each method of device actuation has advantages and disadvantages and proper selection greatly depends on design specifications. Micro pumps driven by piezoelectric actuation[4] and even pumps driven from optomechanically responsive nanocomposite

hydrogels[5] are some examples of integrated micro pumps. For valves, equally different techniques have been developed to stop or redirect the bio-fluid directly. Phase change based valves using paraffin wax have been developed and integrated into microfluidic systems.[6,7] Magnetically driven micro ball valves[8] and electrically driven thermo bimorph valves using a Si-Ni micro beam[9] have been successful and were both considered for use on this project. These valves are able to directly affect the flow of the working fluid through electrical means. Alternatively, the control of the working fluid can be achieved through the use of pneumatically actuated fluid control devices.

The use of pneumatics has been shown to allow for integrated micro pumps, valves and logic structures.[3,10-11] Eddings categorizes pneumatics into three categories based on actuation principles: pneumatic, the use of direct pressure control; thermo-pneumatic, the use of temperature controlled pressure changes; nontraditional pneumatics, the use of positive and vacuum pressure. Pneumatically actuated fluid control devices have the disadvantage of often needing an outside pressure source with accompanying valve devices. If the pneumatic control devices such as valves and air channels were to be miniaturized, then the overall system size of a pneumatically actuated fluidic device could be reduced significantly. Full integration of the pneumatic channels and valves into a chip like device is a step towards miniaturizing the DNA analysis process and developing a portable, robust DNA analyzer.

Motivation

Portability has increasing importance in situations which call for quick, on-demand DNA analysis, such as is required for a pathogen detection device. A portable

pathogen detection device has been developed by Idaho Technology, called the RAZOR.[12] The scope of the project discussed in this thesis is to develop a micro pneumatic valve for use in the RAZOR.

The RAZOR is a portable DNA analyzer developed for military applications. The pathogen sample is inserted into a disposable pouch which contains the chemical reagents needed to analyze the pathogen DNA, Figure 1. The analysis of the pouch is conducted in a permanent housing consisting of pneumatic pumps, valves, hoses and plastic inflatable bladders. The bladders are used to move, mix, and valve the biofluid inside the chemical reagent pouch and are inflated and deflated with the use of three-way valves. Previous work by John Maxwell of the University of Utah developed an Integrated Pneumatic Card, which integrated the pneumatic hoses into channels etched into PCB.[1] This work, however, did not attempt to integrate the pneumatic control valves into the same PCB channels. Integration of microvalves into the pneumatic channels is therefore the motivation behind this project. Successful integration starts with the appropriate method of valve actuation. As discussed previously, various valve actuation techniques exist and many were considered for this project.

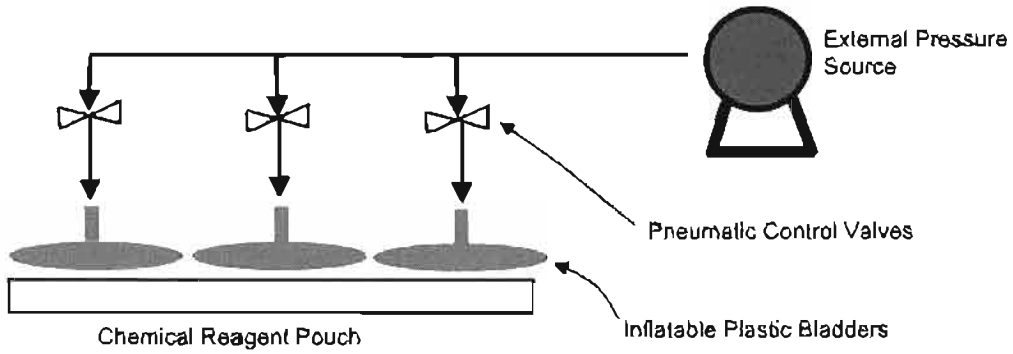

Figure 1. A simplified diagram of the RAZOR processes

Each actuation principle has advantages and disadvantages, and a brief description of considered actuation principles and reasons for their dismissal shall be given here. Micro magnetically driven ball valves such as the one developed by Fu et al. had a relatively large current requirement, 300 mA.[8] This and the difficulty of creating or inserting sufficient coils in the PCB eliminated it and other electromagnetically driven valves from considerations. Paraffin-graphite micro actuators such as the one developed by Ho as well as one developed by Yang et al. had the disadvantage of having a slow response and high power consumption. Ho reported a 3 to 17 second response time with a 200 mW power consumption.[6] Yang and Lin reported a much higher response time of 60 seconds.[7] A Si-Ni Thermo Bimorph actuated microvalve was considered in depth for this application. Yoshida et al. of the University of Tokushima, Japan, reported developing a valve with <0.2 W power consumption, and high through put of 500 ml/min, which made it a possible candidate for this application.[9] However, this type of actuation was not chosen because electrostatic actuation was thought to provide a faster response, lower power consumption and smaller area densities.

Electrostatic Valves

It was anticipated that an electrostatically actuated pneumatic microvalve that used PCB as a building substrate could be quickly, easily, and inexpensively built for this application, as the literature is full of electrostatic microvalves. As a start, electrostatics have been successfully used as type of a clutching and latching mechanism.[13] In 2003, Messner et al. developed an electrostatically driven three-way microvalve for pneumatic applications. This valve was composed on a silicon substrate, operated on 200 V, had a

flow rate of approximately 500 ml/min with a pressure range of up to 10 bar, a power consumption of less than 5 mW, and a response time of less than 1ms.[14] The authors claimed to fulfill the requirements of industry for microvalves, which were given specifically as small size, high flow rate, low weight, low power consumption and short response time. The final size reported for this valve was 16 x 10 x 7 mm^3. It would seem then that this valve had all requirements needed for the RAZOR. The challenge with this valve design was the manufacturability. It was thought that for this application, the use of a silicon substrate and existing micro machining processes would drive the cost and ease of assembly to a point at which the current solenoid valve in use would be more feasible. Cost and ease of assembly therefore became a major factor in the design decision for the development of this valve and is a motivating factor behind the use of printed circuit board as a substrate rather than silicon.

Design Specifications

The need established by Idaho Technology was for a three-way pneumatic valve. The three-way functionality of the valve would allow either the pressure source to inflate the bladders or allow the bladders to deflate to an exhaust port. It was desired that the new pneumatic valve be fully integrated into the small air channels of an Integrated Pneumatic Card composed of PCB layers. Electrostatic force was chosen as the mode of actuation for the new valve and PCB was chosen as the substrate for the valve construction.

Dr. Gale of the University of Utah, working in conjunction with Idaho Technology, developed a list of criterion that a new valve would have to meet to be

considered for a replacement of the current solenoid valves being used by Idaho Technology in the RAZOR device.[15]

1. Valve density of at least 5/cm^2
2. Valve functional at 2 Hz
3. Valve lifetime of at least 10 million cycles
4. Valve functional to 345 kPa back pressure
5. Valve power requirements of less than 0.1 W average power
6. Minimum 50 valve system required
7. Flow rate through the valve of up to 10 l/min
8. Valves integrated into PCB to simplify electronic integration.

CHAPTER 2

THEORY

Overview

The PCB integrated electrostatically actuated pneumatic microvalve operates on simple physical principles. When a potential exists between two conductors, a force is developed between the conductors. The valve uses this electrostatic attraction phenomenon as the actuating force to open and close. A copper foil acts as the valve stopper and is actuated by electrostatic forces which develop between the foil valve stopper and electrodes etched into the PCB substrate, Figure 2.

When the valve stops a flow of air, the static pressure increased inside the valve manifold. Because the exit hole is covered with the foil valve stopper, a pressure gradient develops across the foil valve stopper which results in a force to push the valve stopper against the exit hole.

In the valve, the geometry is such that in the closed position, the foil valve stopper is bent and held down from it resting position. The bent foil valve stopper provides a restoring spring force back to the normally closed position. It will be shown that because of the geometry of the valve, the spring force created from the bent foil flap is small compared to the electrostatic and pressure force. The spring force is therefore negligible and is excluded from total force calculations.

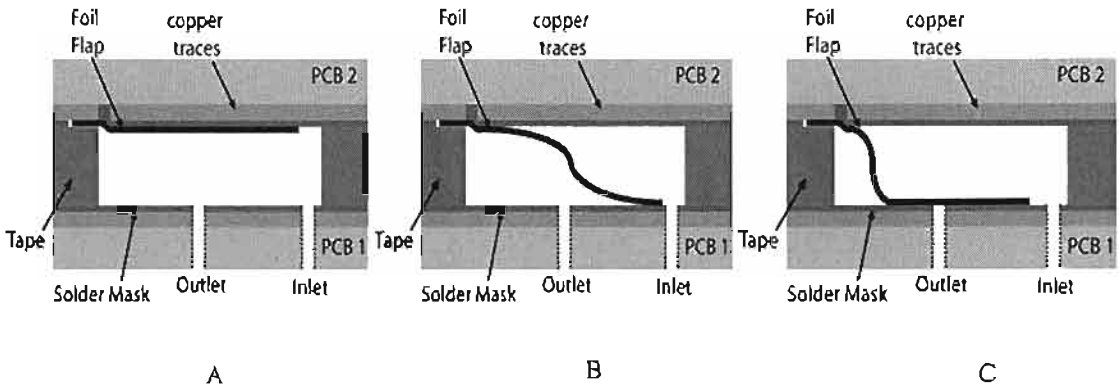

Figure 2. The concept for the actuation sequence of the PCB Integrated Electrostatic Micro Gas Valve. A. A voltage is applied between the trace on PCB 2 and the foil flap to keep the foil in the open position, B. PCB 2 and the foil are short circuited while voltage is applied between PCB 1 and foil. C. Maintaining the voltage bias conditions of B, the foil folds over to cover the exit hole, held by a voltage between PCB 1 and foil valve stopper.

The valve is able to open when the electrostatic force acting on the foil valve stopper is greater than the pressure force acting to push the foil valve stopper against the exit hole. It will be shown that the maximum operational static pressure is a function of the voltage used to actuate the valve.

Valve Design

To meet the design requirements given in the introduction, a valve was developed that could be implemented in PCB and connected to flow channels internal to the PCB. The final configuration of the electrostatic valve was built using layers of double-sided tape, Mylar®, Kapton, copper foil and PCB with the printed circuit board traces and copper foil acting as electrodes, as will be described in more detail in the next chapter. A valve in the designed configuration, Figure 2, is capable of stopping flow in only one

direction. As the design specifications need a valve that can both inflated and deflated (flow in two directions), a three-way valve is needed. By stacking two of the valves on top of each other it is possible to create a three-way valve without increasing the PCB footprint, Figure 3.

The design incorporated 10 valves on one PCB chip, Figure 4. The intent of the valve design was for all 10 valves to share a single pressure source inlet. The 10 valves would then be individually controlled to allow air flow to 10 individual channels.

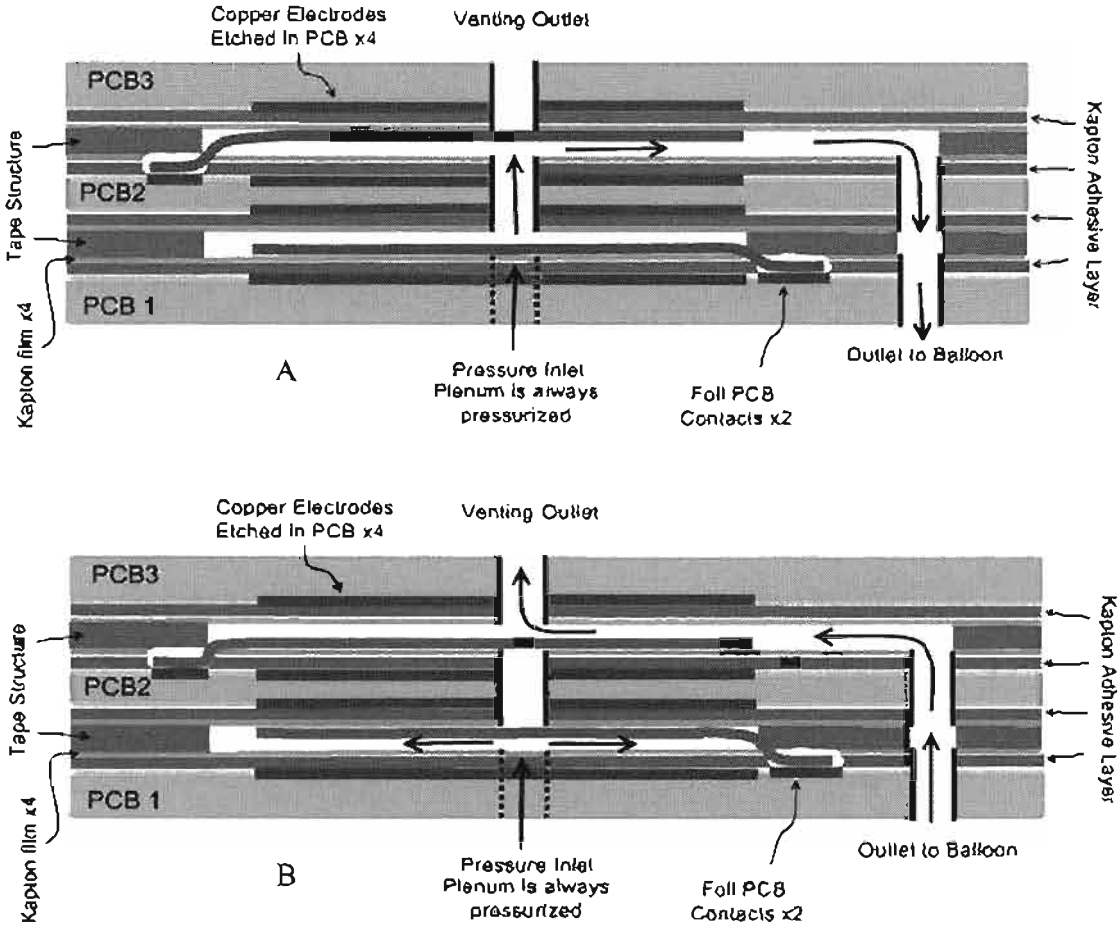

Figure 3. Three-way PCB valve using two one-way valves in stacked configuration, shown in open (A) and closed (B) positions

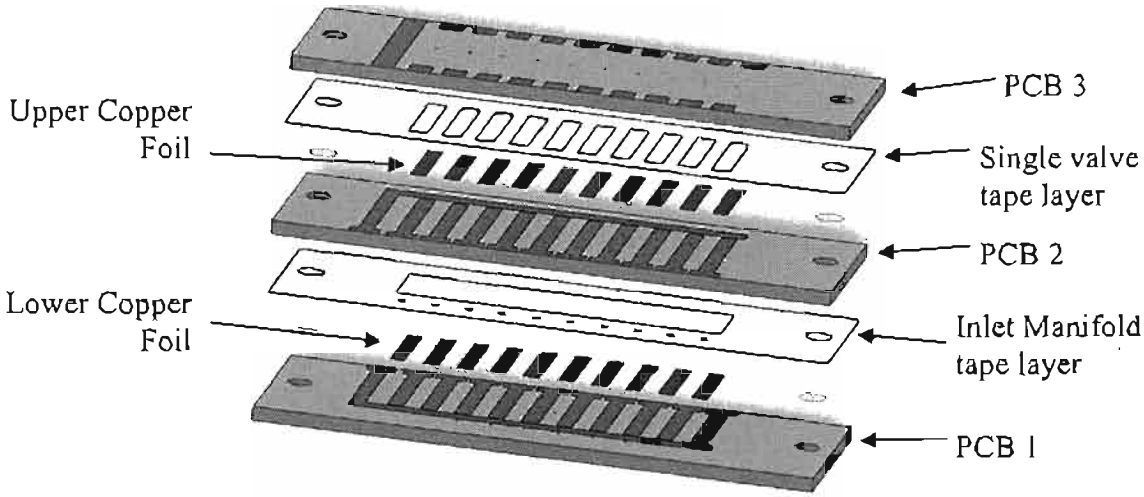

Figure 4. Exploded view of the 3-way valve. Only the lower valve array was built according to this model for testing to prove concept of PCB integration. This figure does not indicate the dielectric used to isolate the foil from the PCB electrode traces.

The lower tape layer, Figure 4, shows a large square cutout that acts as a pressure inlet manifold for the 10 valves.

The three layers of PCB have electrodes and bond pads laid out in the PCB traces as shown. PCB 2 has small holes drilled in the center of the electrodes which have a dual purpose of both being the exit of the lower valve and the inlet of the upper valve, Figure 3.

The copper foil that acts as the flap to stop the air flow through the valve is electrically connected through contact with an exposed trace in the PCB. The trace electrically connects the copper foil flap to a bond pad on the edge of the board. A Kapton insulating layer covers the electrode traces on the PCB. A voltage potential across the copper foil and the electrode on the PCB causes an electrostatic force to attract the foil to the PCB electrode; however it is kept from making contact due to the Kapton

dielectric layer. The electrostatic force acting on the copper foil keeps the foil pressed against the PCB electrodes, covering the small holes drilled in the center and therefore blocking the air path. When the air path is blocked, the flow stops and the static pressure increases. A pressure difference develops across the copper foil, which further presses the foil against the insulated PCB electrode, making the valve more secure.

When the foil flap and PCB electrode have a voltage applied across them, they act as a parallel plate capacitor. As a capacitor, the two electrode plates will retain a charge when the voltage source is disconnected. The charge held on the foil and the PCB electrode will keep the foil in place, whether it is the open or closed position, and the valve will not work properly. To actuate the valve requires a process of applying voltage to the foil and an electrode, then shorting that connection to dissipate the charge before applying a voltage to the other electrode. In the prototype set up, the applying voltage and shorting electrode cycle was preformed with a pair of three-way switch relays controlled by a single manual switch.

To open the valve the copper foil is shorted to the electrodes in PCB 2. At the same time it is shorted, a voltage is applied between the foil and the electrode in PCB 1, which causes an electrostatic force to actuate the copper foil in the opposite direction. This moves the foil to open the air path and allow air to flow. The opening of the valve uses an electrostatic force that must overcome the static pressure force, acting on the foil that developed when it was in the closed position. The spring force created by the bent copper foil flap also contributes to overcome the pressure force, holding the valve to the hole.

In this application, determination of the pressure range in which the valve could successfully operate was found by considering the forces working on the foil flap. In the closed position the foil flap is covering the outlet hole. When the valve opens from this position, the spring force from the foil cantilever flap and the electrostatic force oppose the pressure force keeping the valve closed, Figure 5. Setting the forces equal to zero will produce the relationship between these three forces just before the flap moves

$$F_e + F_s = F_p \tag{1}$$

where F_e is the electrostatic force between electrodes, F_s is the spring force from the bent cantilevered copper foil, and F_p is the force of the manifold pressure acting over the outlet hole.

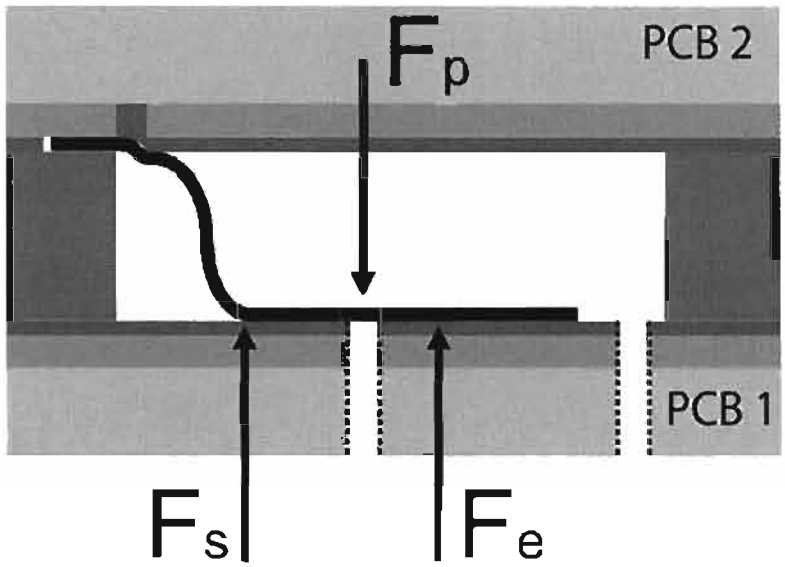

Figure 5. The valve shown is in the closed position and depicted forces acting on the foil valve stopper when the valve is to be opened.

Calculating these forces and their relationship to voltage, pressure and geometry must now be considered.

Electrostatic Force

The operation of the valve is based on the principle of electrostatic attraction. The use of electrostatic forces in MEMS devices is a dynamic process in which the force decreases the distance between the electrodes which in turn increases the force. Thus, electrostatic interactions are nonlinear and require some special attention when modeling. In 2004, Saucedo-Flores et al. studied the effect on electrostatic pull in voltage taking into consideration two dielectrics with different constants.[16] They showed that the electrostatic force of a system with two dielectrics of different constants can be calculated by

$$F_c = \frac{\varepsilon_o \varepsilon_a A V^2}{2(T)^2}, \tag{2}$$

where A is the area of electrode, V is the voltage across the electrodes, ε_a is the dielectric constant of the air space between electrodes and T is defined as

$$T \equiv d - t_d\left(1 - \frac{\varepsilon_a}{\varepsilon_b}\right). \tag{3}$$

In equation 3, d is the total distance between electrodes, t_d is the thickness of the dielectric, and ε_b is the dielectric constants of the Kapton insulating layer. Equations 2

and 3 do not take into account edge effects of the electric field[16] which is a good assumption for this application because of the very large foil flap area compared to the distance between electrodes.

The electrostatic force required to pull the valve flap from the exit hole, thereby opening the valve, is the only electrostatic force of significance in the application. Therefore the electrostatic force will be calculated for the case in which the valve is closed and the distance, T, between electrodes is static and at a maximum value, Figure 6.

In this application there are three different dielectrics: first, the air gap between the foil flap electrode and the Kapton film; second, the Kapton film; third, the adhesive layer attaching the Kapton to the copper trace on the PCB. The adhesive transfer tape manufacture has determined the dielectric constant of the adhesive to be 3.21.[17] It can be shown from the collected data that neglecting the dielectric constant associated with the adhesive layer will allow a better fit of the data to the model. The adhesive layer

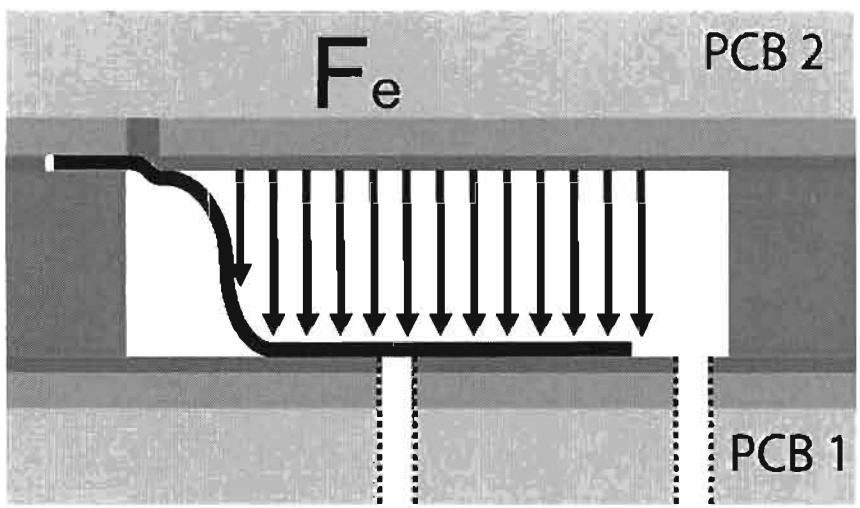

Figure 6. Depiction of the distributed electrostatic force acting on the foil valve stopper when the valve is in the closed position and the shape of the foil valve stopper.

will then be modeled with the dielectric constant of air. The Kapton film is reported to have a dielectric constant of 3.4.[18] Taking into account the Kapton film with equation 2 and 3, the effective electrode distance T is equal to 91.1 microns. Consideration for the different dielectric constant for the thin Kapton film was taken when calculating the electrostatic force of the valve.

Mechanical Spring Force

Determination of Stress in the Foil

When the cantilever beam is fully articulated in the down position to cover the outlet hole, it will exhibit a restoring force to oppose the pressure holding it against the hole. The valve was designed to take advantage of this restoring force and thus aid the electrostatic force to overcome the pressure of the manifold pushing against the outlet hole.

Before the spring force can be calculated, it had to be determined if the foil was acting in the elastic region, thereby validating the use of Hooke's law. The challenge with finding the stress lies in determining the shape of the beam when it is in the fully closed position. To get into this position, the beam is acted on by an electrostatic force between the beam and the lower electrode pulling the beam down. As the beam is pulled down, the distance between electrodes decreases and thus the electrostatic force acting to pull it down will increase. The beam will bend until it reaches the dielectric layer separating the electrodes. Once the end of the beam reaches this layer, it will flatten out and a supporting, normal, distributed force will act to oppose the electrostatic distributed force in that local region relieving the beam of internal bending stresses. The beam will

flatten out along the dielectric layer until it is forced to curve up to reconnect to the point from which it is cantilevered. Once the beam separates from the dielectric layer, the support force this layer provided is lost, Figure 7. At this point, the Euler-Bernoulli beam equations are used to dictate the shape of the beam, given the correct boundary conditions.

Two beam equations were used to determine the shape of the beam, the forces acting on it, and thus the internal stresses in the beam. Since the electrostatic force acting on the beam is a distributed load, the equation

$$y = \frac{wx^2}{24EI}\left(4lx - x^2 - 6l^2\right) \tag{4}$$

for a uniform distributed load was used,[19] where y is the distance the beam has deflected, x is any distance from $x = 0$ at the cantilevered support of the beam to $x = l$ at

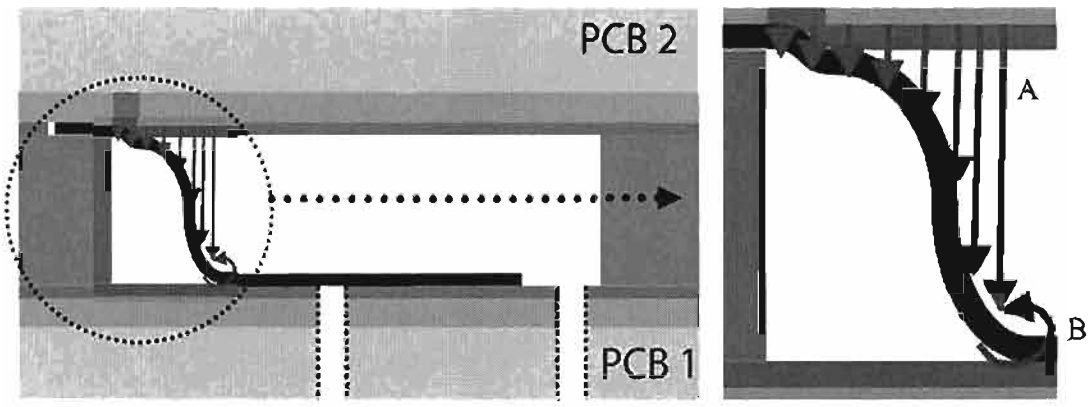

Figure 7. The shape of the foil valve stopper when the valve is closed was modeled as a cantilevered beam with (A) a distributed electrostatic force acting over the length of the beam as depicted in Figure 6, and (B) a moment on one end sufficient to rotate the beam back to zero deflection angle.

the end of the beam of length l, w is the uniform distributed load, E and I are the Young's Modulus and the cross sectional moment of inertia, respectively. Because the beam has an aspect ratio of 200:1, plane strain was assumed thus modifying the modulus, E, by a factor of $1/(1-\nu^2)$ where ν is Poisson's ratio.

Equation 5 satisfies the boundary condition of the beam at length l where the beam must flatten out to zero deflection angle to be able to meet with the portion of the beam being supported by the dielectric layer. A virtual moment can be added to the beam to rotate the deflection angle back to zero. The shape of a cantilever beam with a moment on the end is described by the following:[19]

$$y = \frac{M x^2}{2EI} \tag{5}$$

where M is the virtual moment on the beam needed to rotate it back to zero deflection angle, Figure 7.

Using superposition, these equations can be added together to describe the shape of the beam.

$$y = \frac{wx^2}{24EI}\left(4lx - x^2 - 6l^2\right) + \frac{M x^2}{2EI} \tag{6}$$

By differentiating equation 6 with respect to x, we obtain the deflection angle of the beam at any point x along its length.

$$\theta_{rad} = \frac{dy}{dx} = \frac{12wlx^2}{24EI} - \frac{4wx^3}{24EI} - \frac{12wl^2x}{24EI} + \frac{Mx}{EI} \tag{7}$$

Because equation 4 and all resulting equations are valid for a uniform distributed load only, some assumptions had to be made. The actual distributed load is not uniform and is a function of the deflection, *y*, of the beam. The beam at the cantilevered edge will have a distributed load equal to the electrostatic force calculated at an equivalent distance of 91.1 μm, as given by equations 2 and 3. At the unknown distance *l* of the beam when the boundary conditions dictate a *y* direction deflection of 63.5 μm and zero deflection angle, the distributed load will be equal to the electrostatic force calculated at an equivalent distance of 27.6 μm by equation 2 and 3. The distance of 91.1 μm was obtained from the maximum distance between electrodes when the valve is in the open position and the distance 27.6 μm was obtained from the minimum distance between electrodes. Although the actual equation for the distributed load is unknown, the effects of this nonuniform distributed load can be bound between an upper and lower limit. If it is assumed that the uniform distributed load, *w*, is equal to the maximum distributed load the beam will experience as it approaches the dielectric layer, then this assumption and the resulting stresses, deflections and length, will represent an upper-bound stress state. Conversely, if it is assumed that the uniform distributed load is equal to the minimum distributed load the beam will experience at the cantilevered boundary, then the resulting stresses, deflections and length, will represent a lower bound stress state.

As the beam leaves the cantilevered edge it will take the shape of that described by the lower bound equations for minimum possible *w*. As the beam is deflected and the resulting distributed force is increased accordingly, the beam will approach the shape

described by the upper bound equation for the maximum value of w until it reaches the dielectric supporting layer.

Solving equations 6 and 7 for the virtual moment M and unknown length l can be done with the boundary conditions of $y(l) = y_{max} = 63.5$ microns and $\theta(l) = 0$. After finding the moment M and length of the beam l equation 6 can now be used to describe the shape of the beam when it is engaged in the closed position for both the upper and lower bound cases, Figure 8.

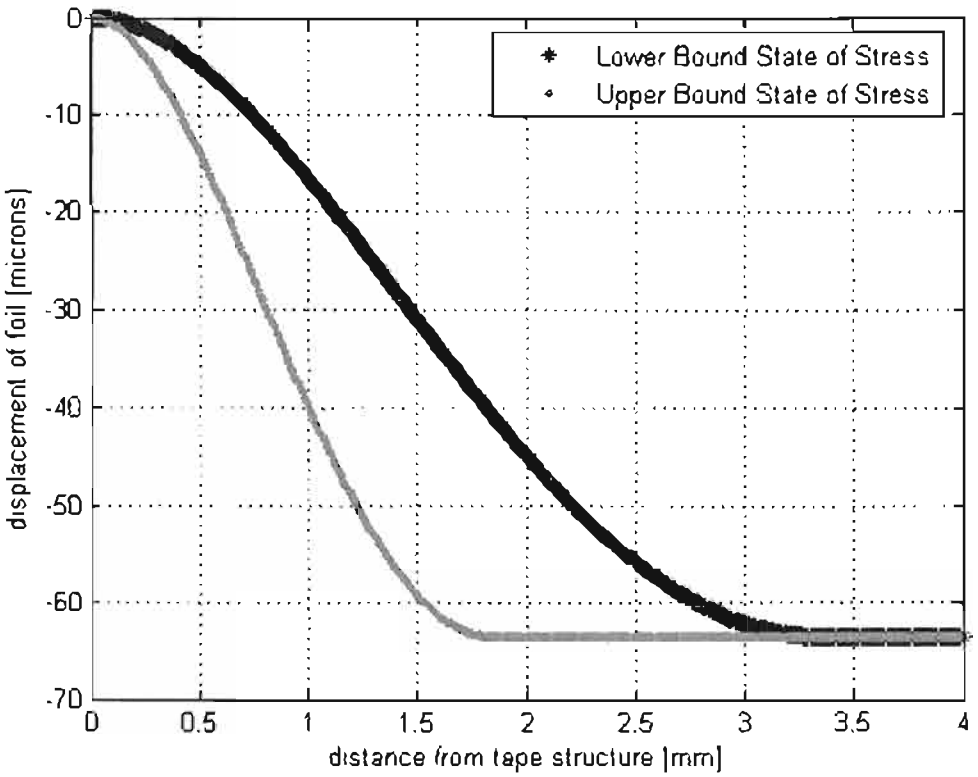

Figure 8. The shape of the copper foil valve flap when it is in the closed position as depicted in Figure 1. The lower bound shape is assumed based on a minimum uniform distributed load caused by the maximum electrode separation distance. The upper bound shape is derived assuming a maximum uniform distributed load caused by the minimum electrode separation.

The aforementioned beam equations have assumptions associated with them as well. One such assumption is that the angle of deflection, *dy/dx*, for the beam is small enough that when placed in the equation

$$\frac{M}{EI} = \frac{1}{\rho} = \frac{d^2y/dx^2}{\left[1+\left(dy/dx\right)^2\right]^{3/2}} \tag{8}$$

it comes close to producing unity in the denominator. For deflections of less than around 5 degrees (0.087 radians), this assumption should yield less than 2% error. To ensure that this assumption holds sufficient for its use in this application, angle θ, or *dy/dx*, was found along the length of the beam for both the upper and lower bound cases, Figure 9. Figure 9 shows that the deflection angle is small enough that the foregoing assumption holds true.

Now that the moment M, distributed force w, and length l are known, the stress in the x direction (lengthwise) in the symmetric beam can be determined with the simplified bending equation

$$\sigma = \frac{M\,c}{I}, \tag{9}$$

where c is half the thickness of the foil beam. The maximum bending moment is at the cantilevered edge where the foil meets the tape structure.

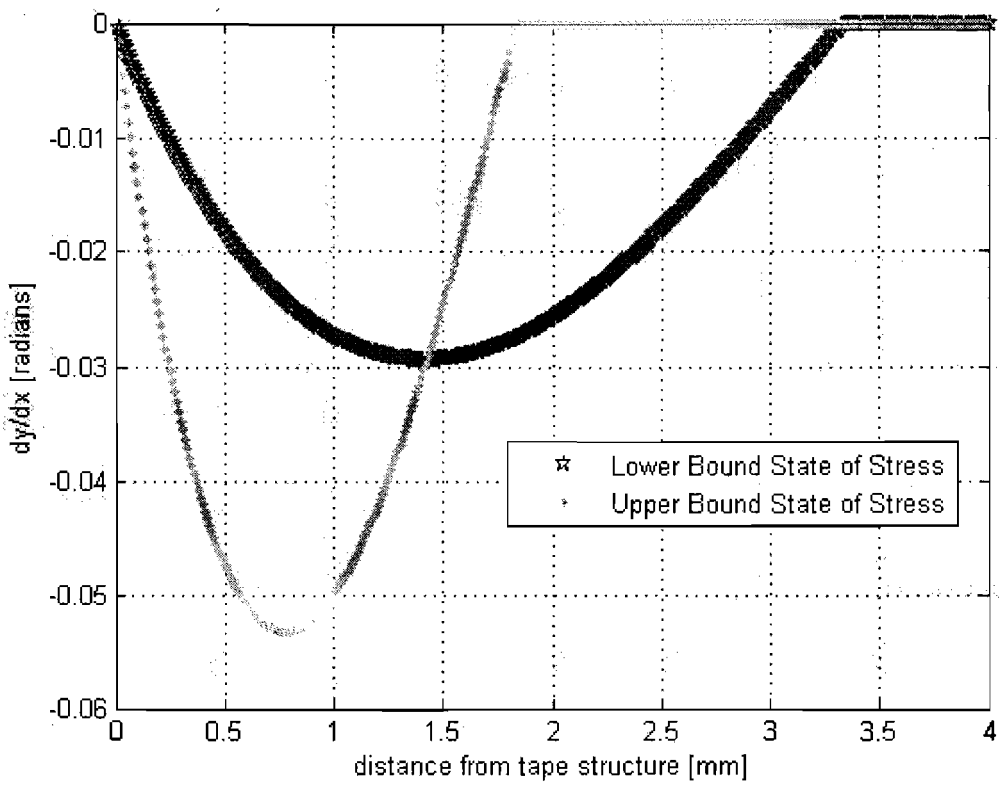

Figure 9. The deflection angle at any point along the copper foil cantilever beam from the fixed tape layer to the point at which the beam contacts the di-electric surface.

Consideration was also given to the assumption that plane strain was in effect causing a stress in the z direction (along the width of the foil) according to

$$\sigma_z = \nu \sigma_x \tag{10}$$

where ν is the Poisson's ratio of the copper foil. Likewise, consideration was given for the average shear stress τ_{xy} determined by the now known w and l. All of these stresses were used to calculated a Von Mises stress and were compared to the yield strength of the copper foil provided by the manufacture.[20] The foil was reported to have a yield stress

of 270 MPa and a tensile strength of 314 MPa, Table 1. This shows that at 488 V the maximum upper limit to the stress seen in the foil flap, will not produce yielding in the copper and it is functioning in the elastic region. If the voltage or displacement y_{max} were increased, the values of M, w, and l would need to be recalculated accordingly.

Fatigue Resistance

It has been shown that the maximum stress in the beam would not produce yielding in the beam material and therefore the beam remains elastic. However, valves are frequently subjected to on-off cycles of operation. Indeed the current solenoid valve for which this valve is to replace is reported to have reliably produced a 50-100 million cycle life.[21] Because the valve flap will be subjected to this bending stress every time it is actuated, fatigue of the metal flap is a concern even if the static load is below the yield strength. To at least get a sense of the fatigue capabilities of the metal valve flap in this type of configuration, a safe life criterion with unidirectional cyclic loading was assumed which gives equal mean stress and stress amplitudes.

Table 1: Calculated maximum stress, spring constant and spring force for the upper and lower bound values of the distributed load w

	Von Mises Max Stress [MPa]	Spring Constant [N/m]	Spring Force [μN]
Upper Bound	82.22	0.54947	34.89
Lower Bound	24.91		

O'Malley notes that copper does not have an endurance limit, but often an equivalent endurance limit is used which is equal to the fatigue strength at 100 million cycles.[22] For copper, this equivalent endurance limit can be estimated to be 100 MPa when the ultimate strength is >280 MPa. This tested endurance limit can be modified to apply more accurately to this situation through a Marin equation,

$$S_e = k_a\, k_b\, k_c\, k_d\, k_e\, k_f\, k_f'\, S_e' \tag{11}$$

in which S_e is the endurance limit of the part, k_a is the surface factor, k_b is the size modification factor, k_c is the load modification factor, k_d is the temperature modification factor, k_e is a reliability factor, k_f is a miscellaneous–effect factor, k_f' is a stress concentration factor, and S_e' is the rotary beam test endurance limit.[19] For this application, only the surface modifier, reliability factor, and miscellaneous-effects modifier were taken into consideration. The above Marin equation reduces to

$$S_e = (.983)(.898)(.9)\ (100\ \text{MPa})$$

The final equivalent endurance limit for the copper foil valve flap was found to be 79.4 MPa. The next logical step is to determine an appropriate fatigue failure criterion and test the endurance limit against the mean stress and amplitude stress. The ASME-elliptic failure criterion was used because it provides a better probability of failure.[19] Using this failure criterion, a fatigue factor of safety was calculated as 1.87 for the upper bound state of stress and 6.18 for the lower bound state of stress.

Spring Force

Now that it is known that the copper is in the elastic region, a spring constant and spring force can be computed through further reducing the model to a cantilever beam and a point force load. Spring constants are related to spring force through displacement with Hooke's law

$$F_s = k\,y \tag{12}$$

To treat the cantilever beam as a linear spring, k needs to be determined for the point at which the force is applied and displacement measured. For this application, only the spring force acting to lift the foil off the outlet hole is desired. Therefore to further reduce the model, it can be assumed that the foil is a fixed cantilever beam with the length l equal to the distance from the edge to the outlet hole exit with some point force acting on the end of the beam sufficient to displace the beam at point l until it touches the dielectric layer, Figure 10. The equation which describes such a system is given as

$$y = \frac{F x^2}{6EI}(x - 3l) \tag{13}$$

where F is the force applied at l. Rearranging equation 13 into the form of equation 12, taking the force to act at $x = l$ and equating coefficients, produces a spring constant

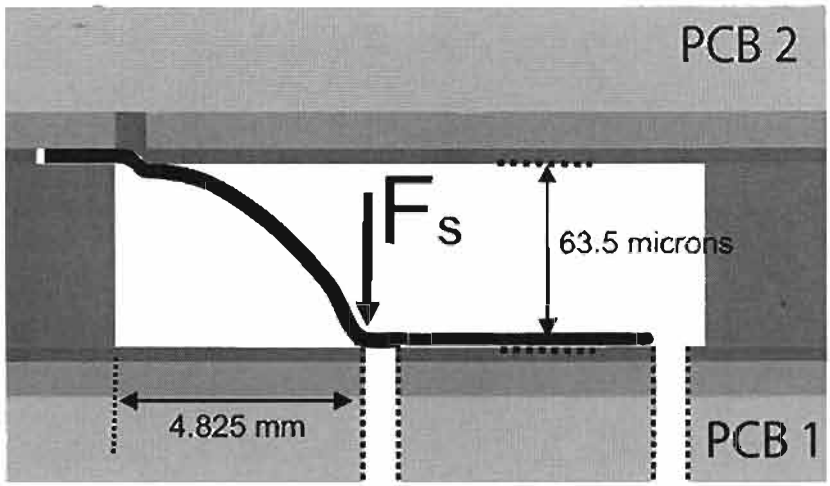

Figure 10. The spring force was calculated using a model of a cantilevered beam of known length and deflection with a point force at the end representing the pressure force pushing on the exit hole.

$$k = \frac{3EI}{l^3} \tag{14}$$

Using a plane strain assumption again for a modified value of E, and taking l to be the distance from the fixed cantilever edge of the foil held by the tape layer to the outlet hole edge and equal to 4.825 mm, equation 14 shows that k is equal to 0.54947 N/m. Therefore, the spring force can be found by applying equation 12 with $y = y_{max} = 63.5$ μm. The spring force, F_s, is found to be equal to 34.89 μN. This is the native restoring force of the metal flap that resists the pressure force, which is acting at the outlet hole. Notice that, unlike the maximum stress in the beam, this spring force is not dependent on the value of the voltage applied across the flap and electrode, and only a function of valve geometry.

The low spring force is not surprising considering the enormous length to thickness ratio of 483. Such a low spring restoring force is an indication that it is negligible compared to the electrostatic and pressure force working on the valve flap. The low spring force is also an indication that the electrode does not need to be so long and skinny and could produce nearly the same results with a short wide beam, so long as the surface area over which the electrostatic force is acting is conserved.

Pressure Force

The pressure force is a rather straightforward calculation. Ultimately what is desired is an indication of how the voltage across the valve electrodes will affect the manifold pressure capabilities in the valve. The only pertinent pressure gradient in the valve is between the valve manifold and the outlet hole when the outlet hole is covered by the copper foil valve stopper. The pressure force can be calculated by equation 1 with the calculated values for F_e and F_s. It has been shown that the value of F_s is insignificant compared to F_e and can therefore be dropped from further calculations. The resultant force from pressure acting over an area can be calculated by

$$P = \frac{F}{A_e}, \tag{15}$$

where A_e is the outlet hole cross sectional area. Substituting equations 2 and 15 into equation 1 and solving for the maximum operational pressure as a function of voltage we find

$$P(V) = \frac{\varepsilon_o}{2T^2}\left(\frac{A_f}{A_e}\right)V^2 \tag{16}$$

where A_f is the surface area of one side of the foil electrode and is equal to 20 mm^2.

Possible Sources of Error

Three possible sources of error occur in equation 16. The area of the electrode foil could possible be larger or smaller than 20 mm^2 and would proportionally change the value of the pressure. However, due to the size of the electrode compared to the size of possible errors in its dimensions, the error associated with electrode size would be rather small.

The pressure is inversely related to the area of the outlet hole. The size of the outlet hole was drilled to 0.35 mm and visually checked with a 0.35 mm drill bit as a go-no-go pin. Due to the size of the outlet hole compared to the size of possible errors, the associated error in the outlet hole could be significant. An increased diameter of just 50 μm would cause a 25% error associated with the pressure. Because a 50 μm diameter error in the valve construction is a possibility, error associated with an increased hole diameter is therefore taken into account when calculating pressure.

The most prominent source for error in equation 16 would be from its inverse square relation to the distance between electrodes. Because of the susceptible nature of the calculated pressure to the distance between electrodes, care was taken during manufacture to maintain thicknesses of the various layers to tight tolerances. Many of the various layers and prototypes were measured with a profilameter to determine their height or flatness. Although care was taken in the construction of the valve, the increase

in height caused by the PCB deflecting under pressure in a balloon type effect was not realized until after data had been collected, as will be shown later.

Because of the unknown magnitude of possible manufacturing error in electrode spacing distance, calculations are base on nominal values and only a possible outlet hole diameter size error of +0.05/-0.01 mm was included in modeling the pressure and voltage relationship, Figure 11.

Power Consumption

The valve is essentially a parallel plate capacitor and acts as such, Figure 12. The capacitance for a parallel plate capacitor is defined as

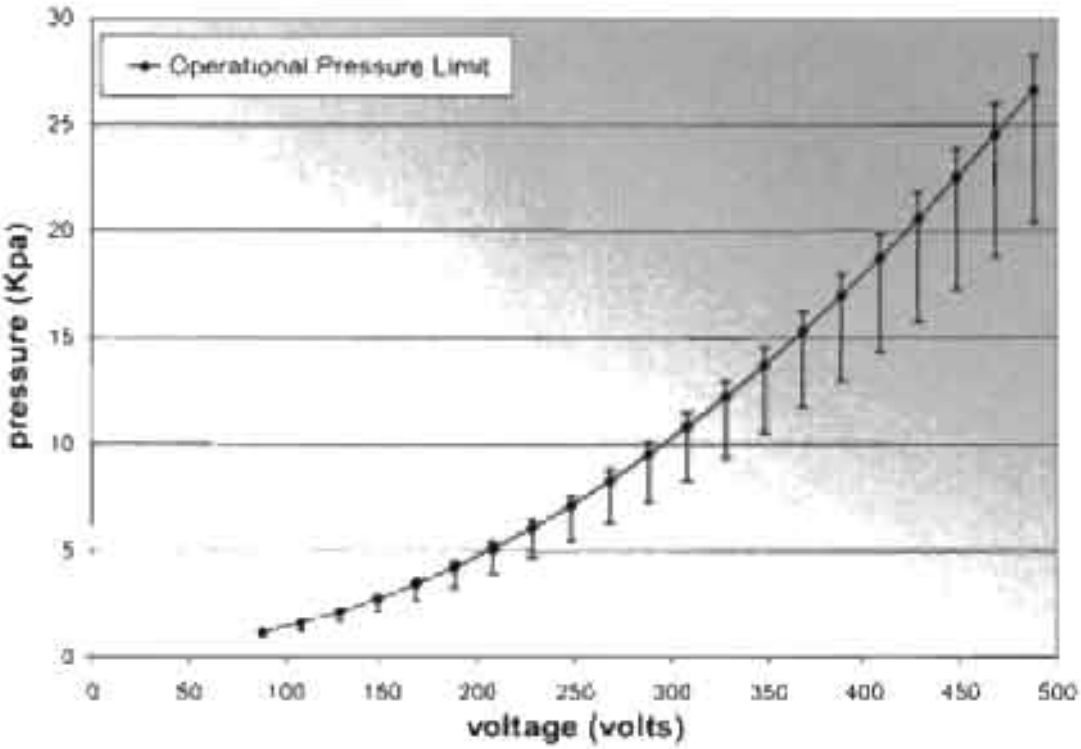

Figure 11. Plot of the theoretical maximum operational manifold pressure as a function of applied voltage

$$C \equiv \frac{\varepsilon_o A_f}{d}, \tag{17}$$

while the energy stored in a capacitor is given by

$$U = \tfrac{1}{2} C V^2, \tag{18}$$

where U is the energy stored in the capacitor of capacitance C at voltage V. because this energy is stored in the capacitor it theoretically does not use power to function. In all capacitors however, the stored charge will remain even after the voltage supply is removed. This stored charge will maintain the electric field and thus the electrostatic force between the foil and the electrode to which it is attracted. Before actuating the flap to the opposing electrode, this charge must be dissipated. Shorting the foil to the electrode to which it is being held is the fastest and easies way to discharge the energy. Therefore this valve must operate with two three-way electric switches to allow for discharging any given electrode to the foil while simultaneously

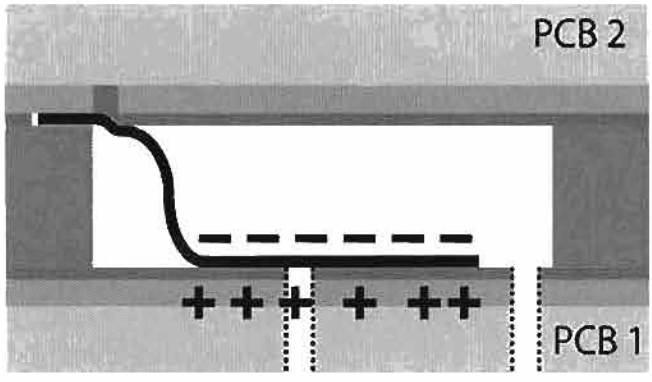

Figure 12. The foil valve stopper is a capacitor and will retain a charge and electrostatic forces after the voltage is disconnected from the valve

applying a potential to the foil and the opposing electrode. This discharging of the capacitor becomes the source for power consumption for this valve. Since the valve must discharge a pair of electrodes before actuating, the power consumption therefore becomes a function of frequency of actuation.

Using equation 17, the capacitance for either open or closed foil position was found to be 17.5 pF. At 488 V and with equation 18, the stored energy in the valve is calculated as 2.09 μJ. The desired switching frequency of the valve and design objective was 2 Hz. The valve is designed such that two discharges and two recharges of the electrodes are needed for one valve cycle. This yields 4 discharges a second for a frequency of 2 Hz. This valve should then consume 0.008 mW of power to maintain this frequency.

CHAPTER 3

MATERIALS, CONSTRUCTION AND METHODS

Overview

As discussed previously, the novel valve is to be made with printed circuit board, double sided tape and copper foil. It was proposed that the use of solder mask applied by the PCB vender would act as the dielectric layer allowing quick and inexpensive assembly of the valve. It was found that this proposal could have potential but due to PCB trace layout flaws, it was not going to work for this prototype. The PCB was found to be unacceptable for this prototype without first being leveled to sufficient flatness. Mylar® and adhesive was used to plan the PCB traces. Kapton and adhesive was used as the dielectric in this prototype.

A sign cutter was used to cut the double sided tape to specifications. The tape outline included alignment holes for proper assembly. Once cut, the tape could be easily assembled onto the insulated printed circuit boards.

The copper foil valve flap was cut with a laser to eliminate edge burrs or creases. The copper foil was cut with alignment marks while on transparent PDMS to allow for accurate and easy assembly.

Once assembled, the valves could be tested. The testing of the valve was to validate the use of the prototype as a valve and to provide general characteristics of the

valve. The tests included testing valve functionality, manifold pressure and voltage relationship, pressure and flow relationships, maximum pressure before leakage, valve cycles to failure, and power consumption.

Initial Functioning Prototype

The first working prototype was created using two glass slides covered in an indium tin oxide (ITO) film to allow for a conductive, transparent surface, Figure 13. Two small holes of 0.25 mm and 0.95 mm diameters were drilled in one of the glass slides for the outlet and inlet, respectively. A layer of Durimide® 284 polyimide was spun onto the glass slides for electrical insulation and measured to be 3.9 μm in thickness.

A single layer of 28 μm (1.1 mil) double sided tape was used to create a channel from the inlet hole to the valve chamber and outlet hole.

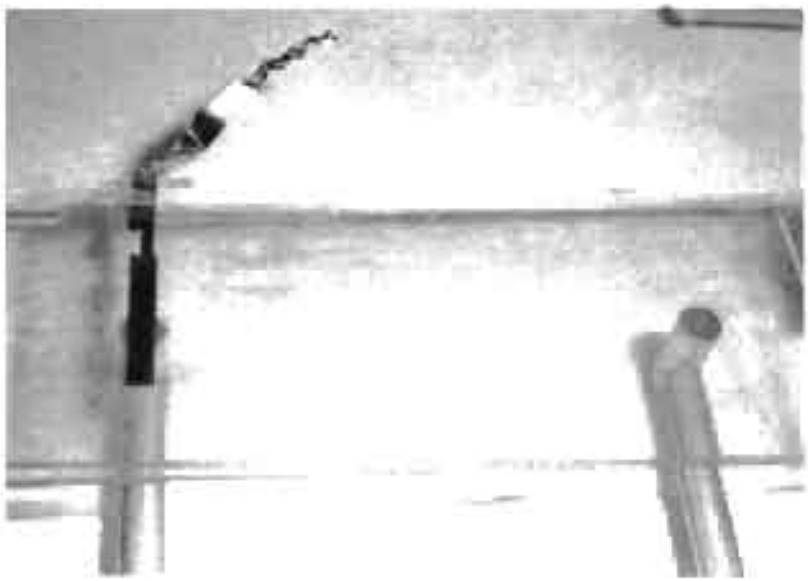

Figure 13. First functional prototype with ITO coated glass slides as upper and lower electrodes and 28 μm (1.1 mil) double sided tape as valve and channel structure.

The lower glass slide was secured to a testing station constructed of transparent acrylic. The gaskets for the inlet and outlet holes were kept independent from each other to eliminate the possibility of cross-talk between the inlet and outlet holes through the development of micro channels in the gasket layer.

An electrical contact was made between the control circuit with power supply and the three electrodes: the copper foil valve flap, and both ITO covered glass slides. Testing of this first prototype was preformed with a micro flow meter and voltage source of 488 V.

This first prototype was a step towards PCB integration of the micro valve. The flatness of the glass slide was meant to reduce possible electric field concentrations. Additionally, the transparency of the ITO covered glass slides allowed for direct visual observation of foil actuation and any mode of failure, if failure should occur. This initial valve did not fail and proved that the use of a copper cantilever foil valve flap was a viable option for an electrostatic actuated valve. Building on the success of this prototype and the insight gained from earlier failed prototypes, a design was devised for a integrated PCB version of the same valve using the same foil flap design. A variation between the PCB and the ITO glass slide version of the valve was the use of the dielectric. Solder mask was desired to be used as a dielectric, as it is already used in the PCB manufacturing process, but, as will be discussed, it was not suitable due to poor PCB trace layout design.

PCB Substrate Preparation

The original design of the valve was based on the intention to compact a reasonable amount of valves into a small chip like structure to allow for maximum valve density while maintaining adequate spacing to allow for the micro channel piping for carrying air to and from the valve. The end PCB design incorporated 10 valves on a single chip. The valves were spaced 4.5 millimeters apart from center to center. The electrodes on the PCB for each valve had to maintain electrical isolation to allow for independently operated valves. The printed circuit boards were to act not only as an electrical circuit component, but also as part of the overall mechanical structure of the valve. To make the valve work, the two printed circuit boards had to be stacked on top of one another. This required the boards to be off center from one another to allow room for wires to be soldered onto the exposed bond pads on each PCB layer. The electrodes them selves were designed to be 2.2 mm by 10 mm. This design would make allowances for small misalignments with the copper foil.

Alignment was thought about a great deal when the valve design was in development. Two 1/8 inch holes were placed on both ends of the chip. The holes were placed in all layers and allowed the layers to slide onto two 1/8 inch brass rods, which, in turn, aligned all layers accordingly.

The PCB was ordered with 2 oz copper traces with a tin coating. Using a Tancor profilometer, the electrodes were measured to be 50 μm +/- 8 μm in height. The height of the electrode traces caused channels to form between the PCB substrate and the tape layer when the valves were constructed. The channels allowed air to leave the valve. This indicated that the height of the electrodes were not negligible as previously thought.

Through various iterative processes and use of a profilometer it was found that using 3M Adhesive Transfer Tape 9458, which is 25 μm (1 mil) thick, and 25 μm (1 mil) Mylar® sheeting, the PCB could be planed to within reasonable levels. To accomplish this planning, the transfer tape was placed on a Mylar® sheet effectively making a Mylar® tape. The Mylar® sheet was then cut using a knife plotter, to the shape of the PCB trace lay out. The cut Mylar® was then aligned, by hand with use of tweezers and a microscope, to plane the PCB. The valves flatness was verified with use of a profilometer, Figure 14.

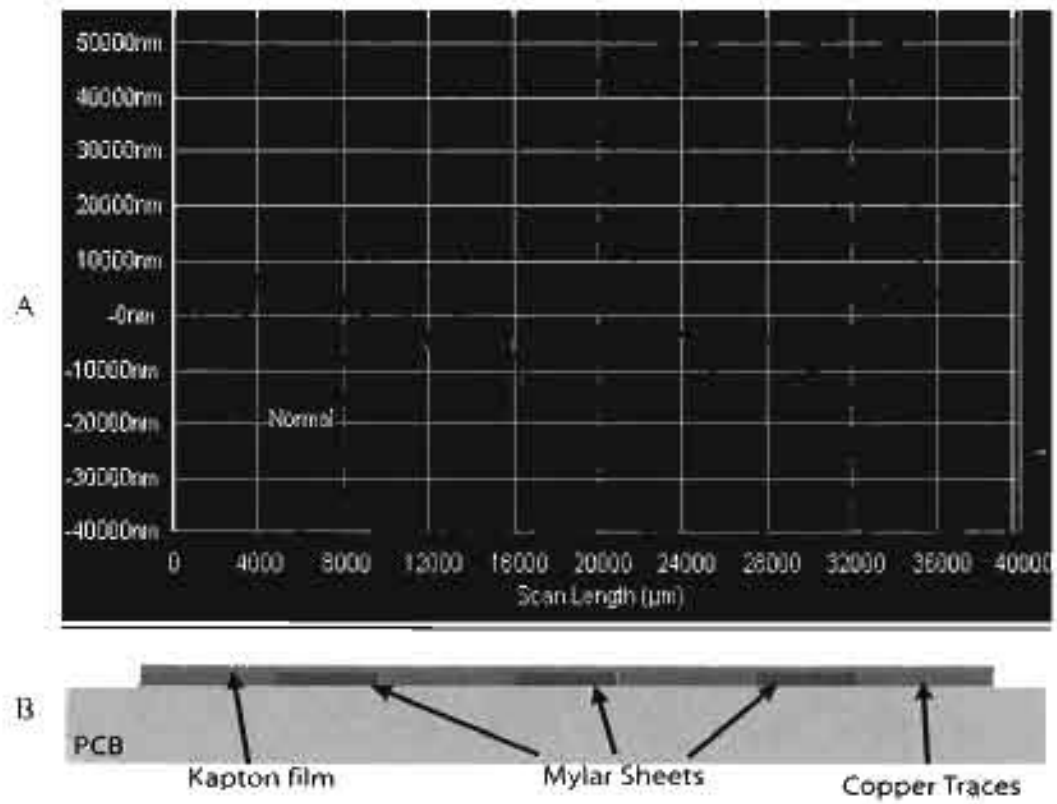

Figure 14. The profilometer measurement of the flatness of the Mylar® planed PCB with Kapton di-electric on the surface. Large bumps are air pockets under the Kapton film, A. Depiction of using Mylar® to flatten PCB substrate, B

Once the PCB was made as flat as possible, depositing a dielectric insulator to prevent short circuits between the PCB electrodes and the metal cantilever was the next step. The dielectric deposition can be done in many ways. Experiments investigating the best insulator for this application involved spinning on SU8, spinning on Fuji Film Durimide® 284 polyimide, use of a common solder mask and use of a Kapton film adhered with various liquid adhesives or 3M Adhesive Transfer Tape 9458. Common solder mask provided the easiest, most consistent, most cost effective, best adhered, and one of the thinnest dielectrics tested. However, because of the overall design of the PCB traces, the solder mask mirrored the undulation of the PCB electrode design and did not allow for a flat surface or for accurate secondary planning of the existing boards. The solder mask would allow the development of channels between traces, which would allow air to leak out of the valves. A better designed board would have solved this problem, but due to budgetary constraints, ordering more boards with a better design to allow solder mask to be used as the insulator was not an option. With this challenge in mind, it was found that a layer of 3M Adhesive Transfer Tape 9458 adhering a DuPont Kapton HN 7 μm +/- 2 μm thin film laid on the Mylar® planed board worked well, with consistent repeatability, for use as the insulating layer.

After the Kapton film was adhered to the flat PCB substrate, the air holes in the PCB had to be reopened as they were covered by the Kapton film. A small drill bit the size of the holes, 0.35 mm diameter, was used to penetrate the Kapton film by hand and allow the hole to be clear of obstruction. The Kapton film and adhesive also had to be removed from the PCB traces, which would eventually make an electrical connection with the copper foil flap to the outside world.

It was shown analytically that a thin dielectric insulator would provide a stronger electrostatic force due to the reduction in the distance between the PCB electrode trace and the copper foil flap. In practice, however, experiments showed that a thin insulating film would provide significant electrostatic forces, but in the areas of the air hole in the PCB, the thin film would often break down. It was found that although the electrostatic force increases with decreasing insulating thickness, the maximum applied voltage is reduced according to the insulating films dielectric strength, which resulted in decreased electrostatic force. There was therefore an optimal thickness for the insulator that provided for maximum force by maximizing voltage according to dielectric strength while minimizing insulator thickness. Kapton film adhered with transfer tape provided ample thickness to allow large voltages before dielectric break down with consistent, cost effective, and easily assembled insulating film.

Copper Foil Preparation

A great deal of effort was focused on what material would be best for the conductive, flexible membrane that would act as the valve stopper. A metal was decided to be the best possible solution for at least a proof of concept. To eliminate possible unintended effects of possible reactions between dissimilar metals, it was decided that because the metal used for the electrode on the PCB was copper, then copper should also be used as the flexible membrane. Two copper foils were experimented with. The first was a standard copper leaf measured to be 4 +/- 1 μm thick. The leaf was very difficult to work with. The leaf would become charged and start to stick to skin, gloves, and just about everything else in the lab. Additionally, the copper leafing could not be cut with

conventional methods used in the lab. Early experiments showed that although the leaf would form a good seal around the air hole, it would tear if the air pressure was too high.

A 10 µm thick copper foil was the second type of copper foil experimented with. The foil could be cut with a knife plotter but doing so left ridges along the edges after being cut. To eliminate the ridges from cutting the delicate foil with a knife, a laser was used to cut the desired shapes out of the foil, Figure 15. The foil needed some way to retain its position after being cut until being assembled in the valve. To help with maintaining position, a thin layer of PDMS was poured on a sheet of Mylar® and cured. The copper foil would electrostatically adhere to the PDMS due to ambient static charges. The adherence of the copper foil to the PDMS allowed the copper to be cut with the laser while retaining position, Figure 15. The PDMS had the additional advantage of being visually transparent, which would aid in the visual alignment of the foil to the electrodes in the PCB. The copper would then be placed in position in the valve and the PDMS layer removed.

Figure 15. The design drawing (A) next to the copper foil after being cut with a laser while being attached to PDMS (B). The two holes that allow for alignment during assembly can be seen on the two ends.

In summary, the copper foil is 10μm thick, 2mm wide and 10 mm long. It is cut with a laser cutter to produce edges that are smooth and free of ridges. The copper foil acts as an electrode and valve stopper and is connected to an outside voltage source through copper traces etched in the PCB.

Tape Structure

The material chosen to build the fluid manifold structure was double sided tape 9492 by 3M which is 63.5 μm (2.5 mils) thick. Double sided tape had been proven by Dr. Gale in previous research projects and was recommended by him for this project. The double sided tape had an advantage of being quickly and easily cut by the knife plotter. The double sided tape used has improved adhesive properties when it is baked according to the data sheet specifications.

To build the tape structure, the tape layer was designed in SolidWorks and cut on the knife plotter to the desired shape. The shape included 1/8 inch holes which would allow the tape structural layer to be aligned and built correctly with the other layers. The tape was cut with the knife plotter and set aside to be assembled with the rest of the valve components. There are two tape layers that act as structure material to build the valve walls for the upper and lower valves in the stacked three-way valve design, Figure 4.

Assembly

The assembly of the valve was done on a custom assembly block. Brass rods 1/8 inch in diameter were inserted into an acrylic block. The first printed circuit board was pressed over the brass rods and positioned on the acrylic block. The next layer was the

tape layer. The tape was slid onto the brass rods and positioned on the PCB layer. The backing was taken off the tape. The PDMS covered Mylar® sheet, which had the copper foil stuck to it, was then slid over the rods and, using a microscope, the copper strips were visually aligned in position. The copper foil would adhere to the double sided tape in position, and because the tape adhesion is much greater than the electrostatic forces holding the copper to the PDMS, the PDMS layer could be gently removed, Figure 16.

Testing Station

To perform these tests a custom testing platform had to be built. The platform itself required several iterations. The final testing station used two acrylic layers adhered together with epoxy.

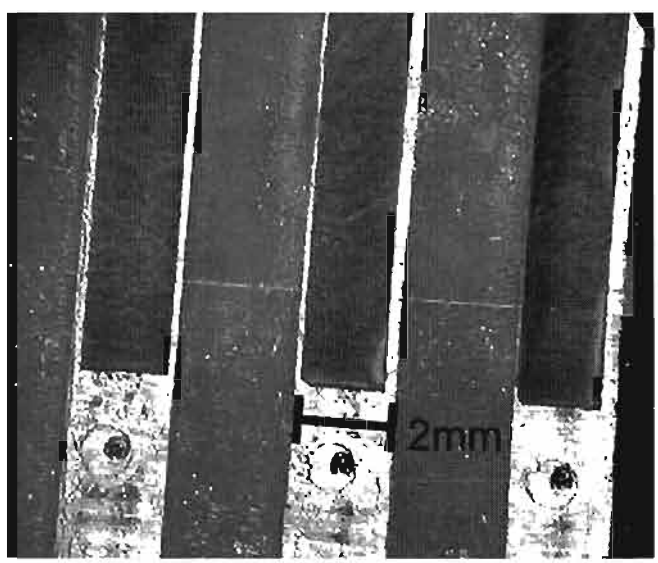

Figure 16. The copper foil valve flap positioned on the double sided tape structure (line across the center of the photo is the valve cavity wall) and is ready for the upper PCB to be placed on top completing the valve construction. The holes across the bottom are the outlet holes bringing the air back to be let out of the bottom of PCB 1 as in Figure 3.

Using a rotary tool, larger channels were routed out of the lower acrylic layer of the testing station allowing for reduced resistance to air flow. The top layer of acrylic was then glued to the lower layer to form the larger channels, Figure 17.

Testing Methods

When designing the valve, several general criteria were given as objectives. These criteria were used to categorize the valve and in part used to determine the tests that needed to be performed on the new valve. The most pressing test performed on the valve was to determine if they could be used as a valve at all, which is to say, if the valve could stop the flow of air. Additional testing included verifying the theoretical operation of the valve by measuring the pressure and voltage relationship, determining the maximum pressure the valve could contain before significant leaks occurred, testing the maximum number of cycles the valve could operate, determining the pressure and flow relationship for the valve, and determining the power consumption of the valve.

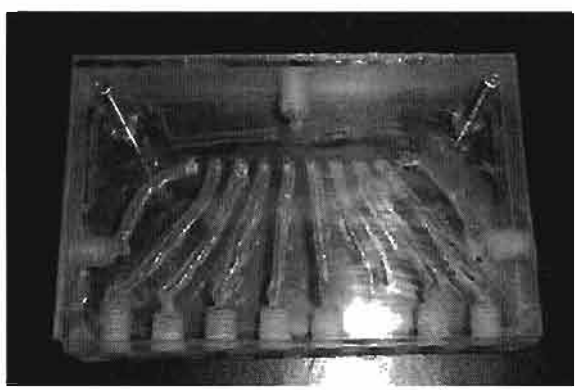

Figure 17. The testing station used to test the valve chips, connecting outside sensors and pressure source to the micro valve manifold and valve exits.

Functionality Test

First the valves had to be tested to determine if they would stop air. A flow meter was hooked up to the output of the valve and the valve was actuated through a cycle. The valves performance was documented. The valve was turned on and placed in the open position. The air was allowed to flow through the valve until it reached the maximum value the flow meter was able to measure, which was 9.125 ml/min. After the valve closed the flow was measured again. The percentage of flow allowed through the valve after closure was recorded. The valves that blocked 100% of the flow were deemed successful and used for further testing.

Pressure and Voltage

According to the theoretical model of the valve, the valve will fail to open if the force on the copper foil from the internal pressure pushing on the foil covered exit hole is greater than the electrostatic force acting on the foil to uncover the exit hole. The exit hole diameter was dilled by the PCB manufacturer and verified by inserting a drill bit through the hole to clear it of possible debris before assembly. When the pressure in the valve manifold was measured, the force on the foil exit hole could be calculated. The foil area was known, the height of the foil from the top electrode was known, and therefore if the voltage was measured, then the electrostatic force could be calculated.

The first test run on the new valves was to vary the voltage and measure the pressure. The voltage was started at 488 V, which was the maximum voltage available from the small DC power supply used for this project. The pressure was increased and the valve actuated until the flow meter registered that the valve no longer opened, at

which point the manifold pressure was recorded. The flow was turned off, and the voltage was dropped by approximately 25 V. The flow was turned back on and process was repeated.

Maximum Pressure

The objective this work was to create a valve that could replace a commercial solenoid valve that could withstand substantial pressure; therefore, the maximum plenum pressure needed to be determined. Ideally the maximum pressure the valve should be able to hold should be determined by the failure of the tape structure resulting in the valve allowing leakage. To test this, the valve and testing station were submerged in a water bath and the pressure was increased slowly. When air was observed to leak, failure of the valve was declared.

Pressure and Flow

The flow meter used to test whether the valve could completely block air was limited to flows less then 9.125 ml/min. To measure flows greater than this, the pressure difference across a small section of straight pipe with known diameter and length was used. The manifold pressure was then varied and the resulting flow was determined.

Knowing the maximum pressure the valve could hold as well as the valve pressure and flow relationship, the maximum flow could be determined. Additionally, since the maximum pressure was determined and the pressure and functional voltage relationship found, the voltage needed to allow the valve to function at the maximum pressure could be determined.

Cycle Testing

The general requirement for the valve was to operate for 10,000,000 cycles. To test the maximum cycles a valve could perform, the valve was operated at 488 V and a pressure that was approximately half of the maximum observed operational pressure at this voltage. A square wave generator was used to actuate a pair of relays that would apply voltage or short the electrodes to cycle the valve open and closed.

The square wave generator was set at 500 mHz, with a correlation between square wave frequency and valve cycle frequency of one to one. A pressure sensor was used to determine the failure of the valve. The manifold static pressure drops when the valve opens. The pressure drop produced a voltage drop that was on the order of one millivolt. The pressure sensor was connected to a computer and recorded with LABVIEW software. When the valve failed, the static pressure would stop fluctuating.

Power Consumption

The power consumption in the valve theoretically depends on the valve cycling frequency. The power was determined by cycling the valve operating at 488 V at a frequency of 2 Hz using the square wave generator while measuring the amperage the power supply saw with an ammeter.

Conclusion

The novel valve prototype used was constructed with PCB, double sided tape, adhesive transfer tape, Kapton and copper foil. Common PCB solder mask was found to be an excellent dielectric for use in this valve; however due to PCB trace layout design

drawbacks, an alternate had to be used. The PCB was planed with adhesive and Mylar® so as to allow the PCB to be as flat as possible. Kapton with adhesive was used as the dielectric layer used to insulate the electrodes.

The double sided tape structure was cut with a knife cutter. The tape structure was 63.5 μm thick. The tape structure created the inlet manifold for the valve chip array. The double sided tape layer was also used to hold the copper foil valve flap to the PCB trace which electrically connected the foil to the out side voltage source. The copper foil valve flap was cut with a laser to eliminate edge burrs or deformations that would keep the flap from sitting flush against the exit hole. Several tests are proposed to validate the functionality of the valve and the theoretical relationships that dictate the valves operational mechanisms. The tests include testing the valve functionality, the maximum operational pressure and voltage relationship, maximum manifold pressure, cycles to failure and power consumption testing.

CHAPTER 4

TEST RESULTS AND DISCUSSION

Overview

The proposed tests discussed in Chapter 3 were preformed on two separate valve chip arrays that had the same construction method and materials. The initial prototype built with ITO glass slides was tested only for functionality before a PCB integrated valve was constructed. The valve was tested to verify functionality, operational pressure and voltage relationship, pressure and flow relationship, maximum pressure, cycles to failure and power consumption.

A digital pressure sensor was used to measure the manifold pressure. A multimeter was used to measure the voltage applied to the valve through a high voltage DC power supply. The maximum operational pressure and voltage relationship developed in Chapter 3 was validated and verified to be of the correct form. LABVIEW was used to record the cycles to failure test. The cycles to failure test was conducted on three valves. The three tested valves appeared to have failed for similar reasons and operated for several thousand cycles. The maximum pressure the valve was able to withstand was found to depend on the double sided tape layer and was significantly greater than the maximum operational pressure the valve was able to operate given the

voltage. The power consumption was tested and resulted in a consumption that was greater than expected. Each test result is provided and discussed at length.

Valve Functionality

The initial prototype built with transparent ITO film covered glass slides was not fully tested as it was a step towards the desired PCB integrated version of the valve. This ITO version of the valve was tested only for its flow blocking capabilities. It was tested with the same micro flow meter used to test the PCB integrated valve. The ITO prototype was tested at 488 V and was found to block 100% of the flow registered on the flow meter.

After a single valve chip was fabricated as described, it was tested for its ability to block air. After it was proven to work for one chip, one more chip was made with the same manor to show repeatability. The second chip was created and worked with similar performance, Table 2. One hundred percent of air flow corresponds to 9.125 ml/min as read from the flow meter and tables provided by the manufacturer. The numbering scheme on the valve is such that the first number indicates the chip followed by a number to indicate the valve on the chip.

Voltage and Pressure Relationship

The theoretical operation of the valve presented in Chapter 2 shows that the ability of the valve to open is dependent on the balance of forces from the pressure acting over the exit hole area and the electrostatic force between the top PCB electrode and the foil.

Table 2: Percentage of air blocked by two valve chip arrays that had the same construction procedures and materials.

Mylar® planed, Kapton insulated		Mylar® planed, Kapton insulated	
Valve	Percentage of air blocked	Valve	Percentage of air blocked
4.1	10.5%	6.1	98.8%
4.2	100.0%	6.2	98.0%
4.3	100.0%	6.3	93.9%
4.4	100.0%	6.4	100.0%
4.5	100.0%	6.5	96.0%
4.6	100.0%	6.6	97.3%
4.7	100.0%	6.7	92.7%
4.8	22.6%	6.8	95.0%
4.9	16.4%	6.9	92.1%
4.10	5.0%	6.10	84.2%

The relationship between the voltage, which controls the electrostatic force, and the valve manifold pressure, which controls the pressure force, needed to be determined experimentally to validate the theoretical model of the valve actuation.

The valve manifold pressure was measured with a digital pressure gage and was taken at the connection of the pressure source to the valve testing fixture. The voltage was changed and stepped in 25 V increments. The pressure source was turned on and the valve was actuated. The pressure was then increased as the valve actuated. When the valve could no longer actuate it was concluded that the static manifold pressure was the

maximum pressure that the valve could hold at that particular voltage. This process was repeated for each fully functional valve over a reasonable range, Figure 18. The theoretical relationship between electrostatic force and voltage is inversely proportional to the square of the distance between the top electrodes and the copper foil.

As the pressure increased in the manifold, the top PCB board would be forced to separate from the lower board in a balloon type effect which would increase the distance between the top electrode and the copper foil. This phenomenon would cause the electrostatic force used to open the valve to be diminished which would explain the smaller than expected readings.

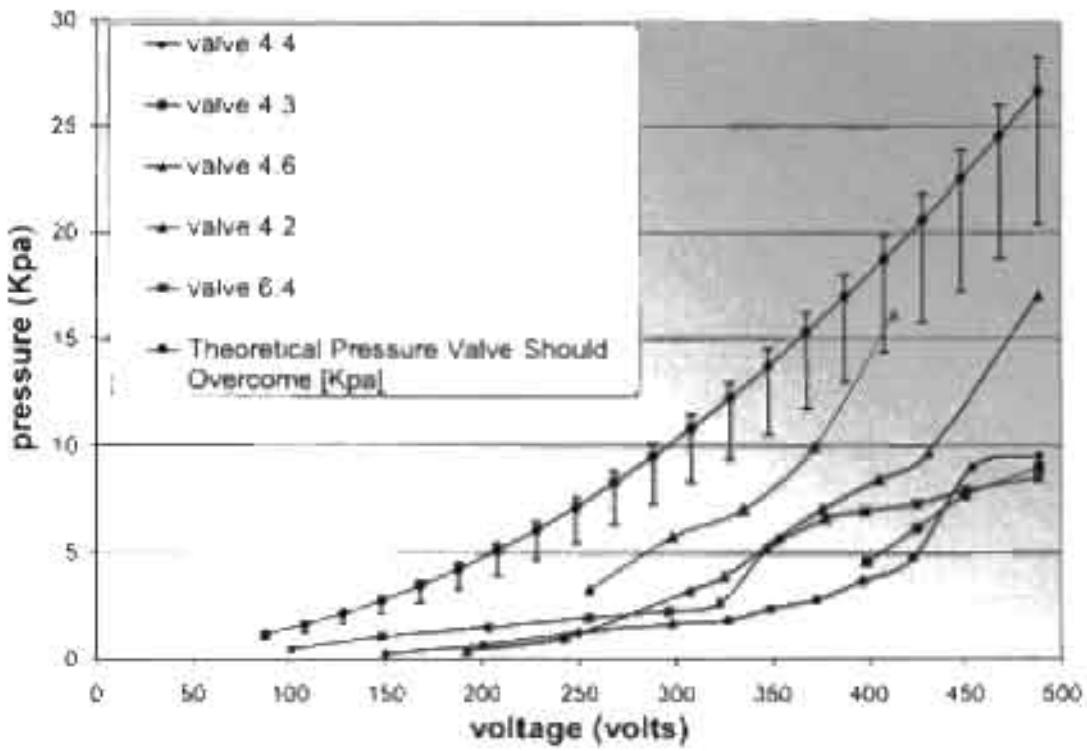

Figure 18 The experimentally collected pressure and voltage data plotted with theoretically expected results.

To diminish the effects of this phenomenon, the valve was compressed just as it was when first manufactured between each voltage and pressure data point acquisition. As the distance between electrodes grows, the parabola describing the relationship between pressure and voltage widens. If the distance between electrodes expanded due to the ballooning effect, then the line describing the theoretical pressure would start to flatten out and the collected data would near the theoretical band. If the distance between electrodes were increased by 40 microns, which is less than the thickness for a piece of paper and would be reasonable for this application, considering the pressure and relatively weak adhesion of the tape layer, the theoretical model would show almost as a trend line for the collected data, Figure 19.

A very interesting phenomenon was observed while collecting data. When the valve was in the off position and no flow was measured, the manifold pressure would increase and stabilize to some value. After the valve opened the manifold pressure would decrease as fluid began to flow. As the pressure, however, approached the limit for a particular voltage, the opening of the valve began to exhibit interesting changes. The pressure would slightly drop and a minute amount of flow would be measured for a brief moment before the flow would suddenly increase to the fully open valve condition and the pressure would drop to a level consistent with this type of flow.

This observed delay in actuation was observed to increase slightly with increased pressure, until the pressure reached a maximum for that given voltage and the valve would no longer open. The cause for this delayed response is thought to be caused by the imbalance of per area forces acting on the valve foil flap.

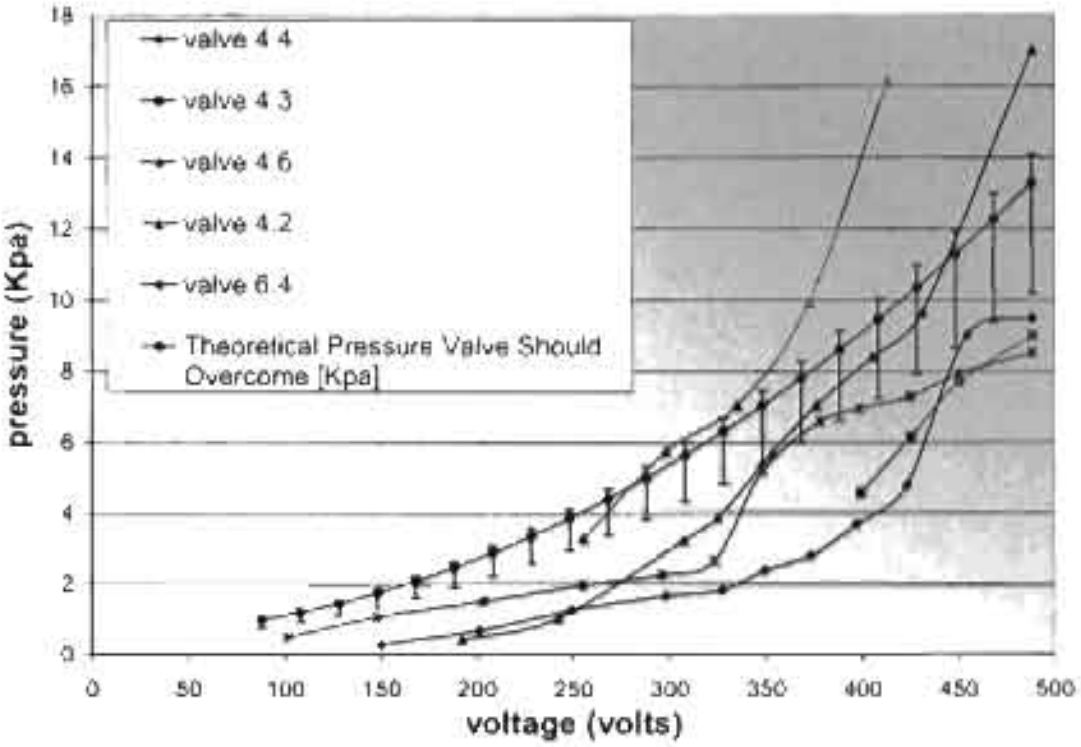

Figure 19. Collected pressure and voltage data with ballooning effect accounted for. A ballooning effect was observed as the manifold was pressurized. If an extra 40 μm of PCB distance was accounted for, the theoretical results would fall in the middle of the collected data.

Although the force opening the valve was greater than the force keeping it closed, the two forces were acting on different size areas, the electrostatic force acting over the entire foil flap while the air pressure was acting over only the outlet hole region. This should cause the foil to take the shape of a flexible membrane with a large point force acting in the middle. In this shape a small opening could be created near the outlet hole edge, allowing a small amount of air to flow. As this small amount of air flowed, the static pressure would drop and resulting force holding the foil to the hole would decrease. This would allow the valve foil to then snap suddenly down, resulting in the sudden increase of flow and decrease in manifold pressure that was observed.

The trend of each of the valves demonstrates a relationship that is consistent with what is expected in the theoretical model. The theoretical model predicts the relationship of the electrostatic force used to open the valve being proportional to the square of the voltage applied between the top electrode and the copper foil. Considering the rough manufacturing methods, I think that this is rather encouraging for future work and shows promise for a PCB integrated, electrostatic actuated gas valve.

Pressure and Flow Data

Pressure and flow data are important to valves for various reasons. Pressure and flow data are important to engineers to determine the head loss across the valve. To determine the flow through the valve, the pressure drop across a small, straight, smooth tube was measured. For experiments with a flow below 9.125 ml/min, a flow meter was used, but generally the valves were found to work properly under flows greater than this. To find the flow to manifold pressure relationship, the pressure drop across a small smooth pipe was used

$$\Delta P = \frac{32 L \mu \overline{V}}{D^2}, \tag{19}$$

where L is the length of the constant-area, straight, horizontal pipe, μ is the viscosity of the fluid, V is the average velocity of the fluid, and D is the diameter of the pipe. The small pipe was 128 mm long with an inside diameter of 0.65 mm. From this relationship the average velocity of the fluid was found and therefore the volumetric flow rate of the fluid. One valve was tested to determine the pressure and flow relationship, Figure 20.

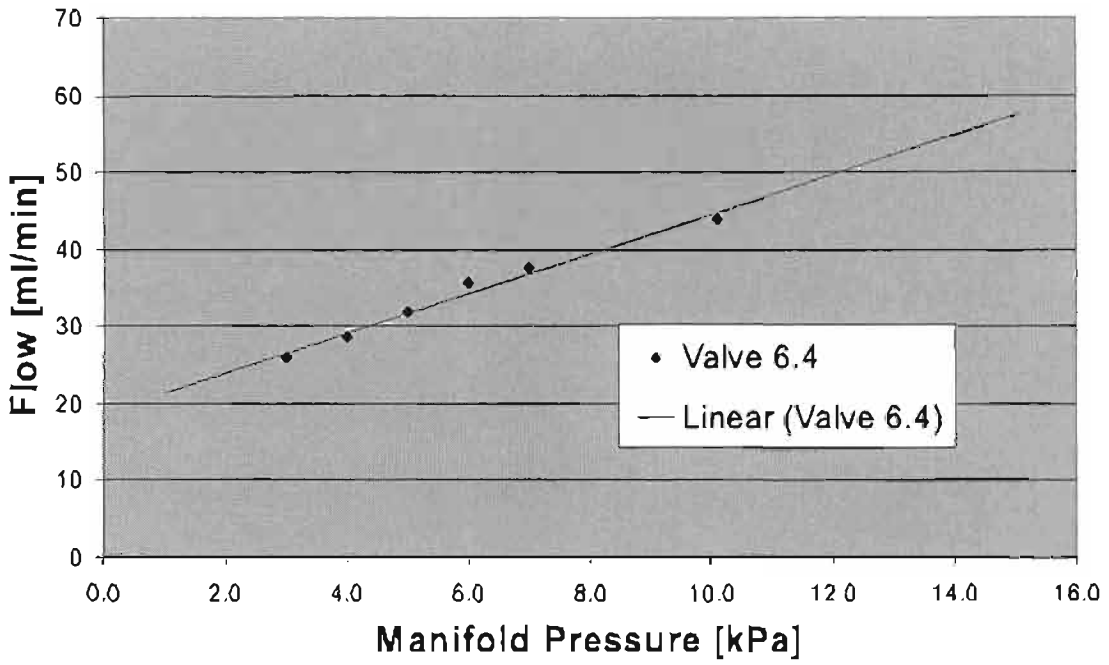

Figure 20. The flow through a single valve with respect to the manifold pressure

One of the major challenges with accurate classification of the pressure drop across this valve is in the design of the valve chip array. The 10 valves share a single pressure manifold with one input in the center of the manifold between valves 5 and 6. The problem with this design lies in the manifold. The valves farther from the single shared inlet will have a higher pressure drop because the air must travel through the micro plenum of only 63 μm (2.5 mils) in height, which causes significant friction losses, before it reaches the valve outlet, Figure 21. The flow measurements were direct measurements with a flow meter.

Because of the large inconsistencies involved in determining the pressure drop across an individual valve stemming from design drawbacks, the pressure and flow data

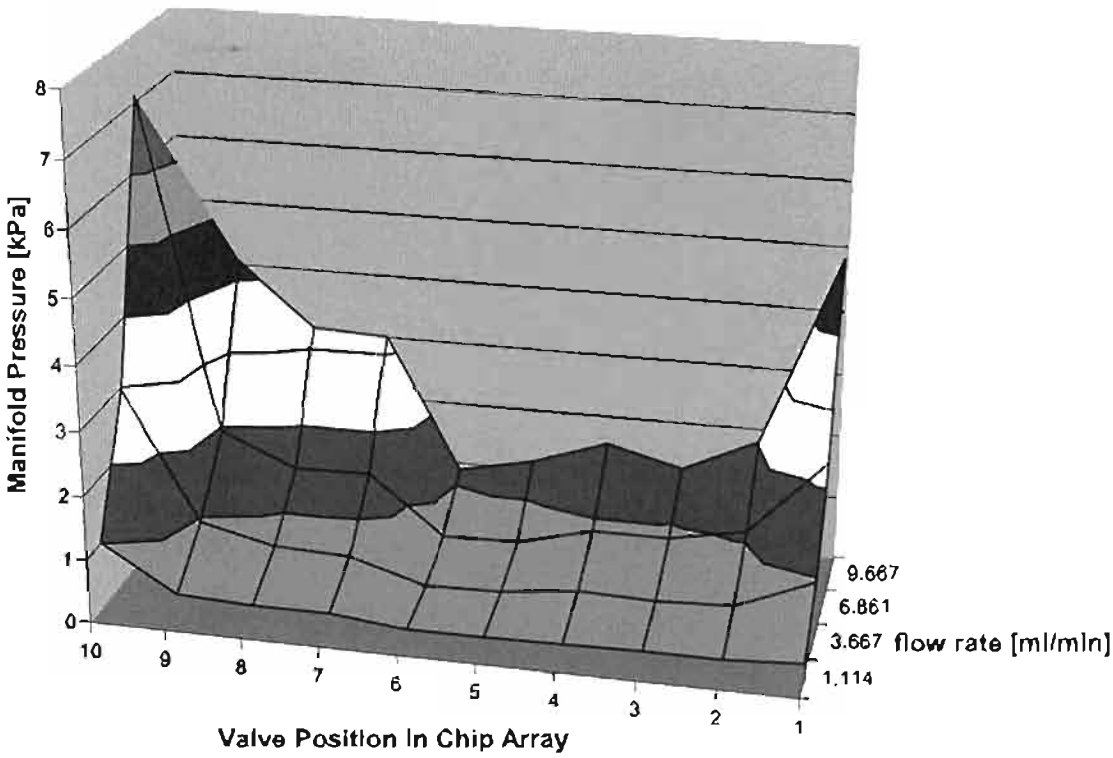

Figure 21. The mapping of flow rate with respect to manifold pressure and valve position on the chip array. The inlet is in the center of the manifold between valves 5 and 6, each valve has an independent outlet.

presented in Figure 20 and 21 should therefore be considered qualitative in nature for the shared pressure inlet manifold valve chip array design.

Cycle Testing

The number of cycles a valve can endure before failure is an important engineering criterion and can be found as a selling point on many commercially available valves including the valve currently in use by the RAZOR. It was desired that this design would have a cycle life of at least 10 million cycles.

Three valves were tested to failure using a circuit that incorporated two relays powered by a square wave generator. The relays would either apply voltage or short circuit electrodes depending on if the valve was opening or closing. The test used 488 V applied to the valve electrodes and operated at a pressure that was approximately ½ of the average maximum pressure the valves could operate for this voltage. The valves were cycled at a rate of 500 mHz. Because the manifold static pressure would increase when the valve closed and decrease when the valve opened, the manifold static pressure was used to determine if the valve had failed. The pressure was recorded by LABVIEW.

The first valve tested was valve number 4.5. The test was started at 11:05 am on 20 Oct 2008 with data being recorded by the computer. It was observed to function correctly at the time the test was started. It was observed to still be functioning later that day. The valve was left to cycle and the computer was left to record data through the rest of the day and into the night. It was observed to still be functioning at 1 am on 21 Oct by a lab staff member. At 10:30 am on 21 Oct the valve was observed to have failed. Due to a technical issue with the data collection computer, the data for this test were lost sometime during the night. It was found that failure of the valve did not affect the function of the adjacent valves.

The second valve tested was valve number 4.4. The test was started at 1:30 pm 21 Oct 2008. It was last observed working at 11:15 am 22 Oct with no apparent degradation to the valves ability to block air. At 11:56 am 22 Oct it was observed to have failed, but due to excessive ambient signal noise in the data it was unclear as to the time of failure. The failed valve was observed to have the same response as the first failed valve.

The third valve tested was valve number 4.2. The test was started at 10:30 am 23 Oct. The signal from the pressure sensor was put through a voltmeter that filtered the noise and allowed a clean record of the pressure sensor voltage. The valve was observed to function properly at the start of the test and throughout the test. After failure, the valve was observed to exhibit a similar response to the first two failed valves, Table 3.

All three valves appear to have failed for a similar reason. The data collected from the third valve show a consistent pressure change to coincide with the valve's opening and closing cycles from the start of the test until a sudden and complete failure, Figure 22.

To make sure the failure was complete, the valves were completely disconnected from pressure and voltage sources and then reconnected and attempted to operate. The valve did not operate again and produced the same results which showed the failure was total.

Table 3. Measured number of cycles to failure of three fully functional valves. These valves were cycled at 500 mHz until catastrophic failure.

	Valve 4.5	Valve 4.4	Valve 4.2
Hours of Observed Operation	13.92	21.75	25.77
Observed Minimum Number of Cycles	25050	39150	----
Observed Maximum Number of Cycles	41400	40380	46378

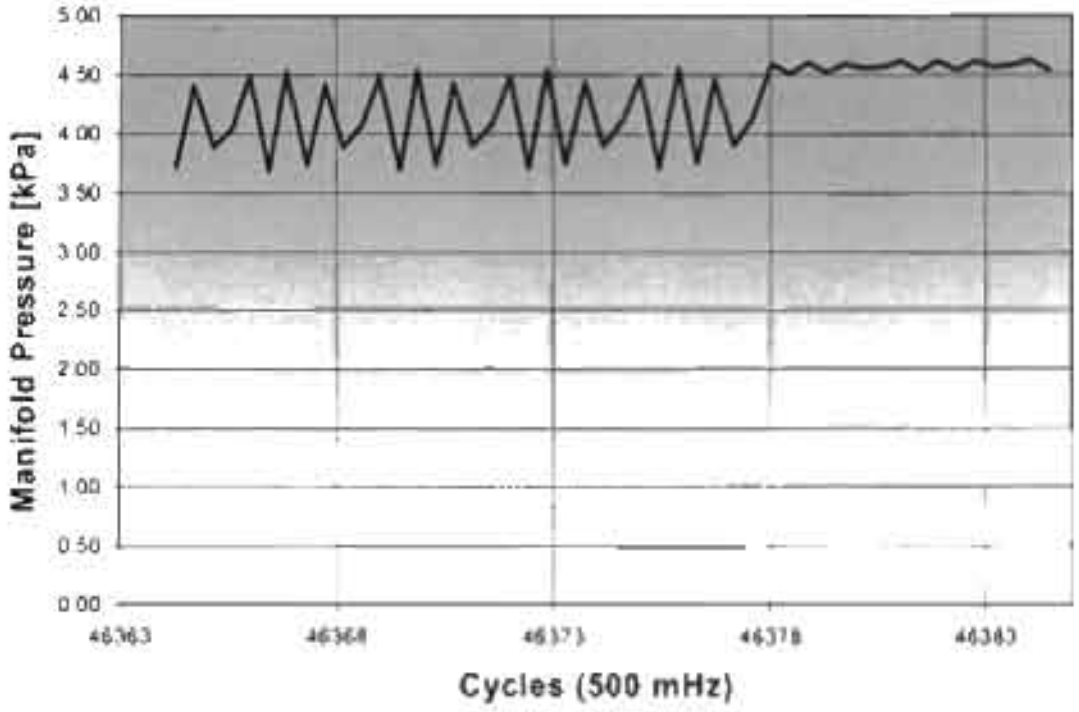

Figure 22. The manifold static pressure as the valve actuated at 500 mHz. This shows the point of valve failure. All data before this plot had the same pattern, which indicates failure was sudden and complete.

A voltmeter was attached to the valves and it was found that no short existed in the valve. An ammeter was then connected to the valve circuit and voltage applied. No current was registered, which indicates that no arcing was taking place within the valve. Pressure was applied to the valve and flow was measured. The voltage was then removed from the valve which would allow the foil flap to be free to flutter or act freely according to the air flow around it. No change in pressure or flow rate was measured.

Upon opening the valve chip, the chip was destroyed in the process. The foil flaps were found to be completely intact, which therefore rules out the possibility of failure due to mechanical fracture of the foil. Additionally, no corrosion product was found on the foil, nor was debris found in the outlet of the valves that failed.

The failure of the valves is consistent with a failure in the electrostatic field, which is maintaining the valve in the open or closed position. Additionally, the connection between the foil flap and the outside voltage source is only a press fit between the tape layer and the lower printed circuit board traces. It is then concluded that failure was due to an electrical separation between the foil flap and the PCB trace that delivers the potential to the flap. An improved design could eliminate the need for a press fit electrical connection and therefore extend the life of the valve.

Although this cycle test did not conform to ASTM standards for determination of the cycle life of automatic valves for gas distribution system components,[23] the similarity of the results across the three tested valves and the relative longevity of the valves themselves, being prototypes, should indicate that this valve design could hold significant potential as a automatic gas valve for PCB integrated pneumatic systems.

Maximum Pressure

An immediate design drawback to this valve is the use of double sided tape for the valve structure. Due to the inexpensive nature and ease of manufacturing when using the double sided tape as a building structure, it was considered for the primary building material for proof of the valve design.

The double sided tape allows quick prototyping of a fairly accurate micro structure for channels. The success of the tape as a microchannel and as a sufficient valve structure building material was proved in the first working prototype of the valve, which used transparent ITO glass slides in place of opaque printed circuit boards. Finding the maximum pressure this tape structure could successfully hold in the manifold

was important to determining the maximum flow rate the valve could successfully allow when the data were coupled with pressure and flow data as discussed. It was also important to understand the manifold pressure structure capabilities to give a sense of the minimum voltage that needed to be applied before foil flap actuation becomes the limiting factor to valve pressure capacity.

Valve chip number 6 was attached to the testing platform and all voltage source wires disconnected. A pressure source hose was connected to the inlet and a venting hose was attached to the valve 6.4 outlet. The test platform with valve was then submerged in a water bath and pressure was increased to normal functional pressure of approximately 8 kPa. No leaks were detected at this pressure. The pressure was then slowly increased over a matter of minutes until leaks could be observed, Figure 23.

Figure 23. The failure of the valve structure wall after being tested submerged.

At 197 kPa (28.57 PSI) bubbles were observed to come form the side of the valve, from the tape layer. The small bubbles quickly grew into in to large leaks as the manifold was allowed to linger at this pressure. This pressure is then concluded to have failed the tape structure.

The ASTM standard for cycle testing automated gas valves has stipulations for pressure increases at specified increments.[23] Although this test did not conform to such standard, it is informative in that it provides a view at the limitations of the tape structure on this valve design. The pressure the structure can withstand is related to the adhesion between the tape and the printed circuit board which can vary with an improved design. A design change, which is recommended, would therefore need to be retested.

Power Consumption

To measure the power consumption of the valve an ammeter was hooked up in the valve actuating circuit. Theoretically the valve is not going to consume power until it is actuated from open to close at which time the stored energy in the foil flap and the electrodes would be discharged. The valve was cycled at 2 Hz and 488 V and as expected the current flow fluctuated as the valve plates charged and discharged. The ammeter registered 0.009 mA peak current. A square wave was assumed because of the calculated capacitance time constant of the valve was less than a micro second. The short time constant of the parallel plate capacitor, which is what the valve essentially is, means the transient portions of the charging and discharging cycle are negligible compared to the relatively large amount of time the plates are fully charged or fully discharged. Taking the root mean square of this amperage gives .0045 mA of current. This will give

a power consumption of 2.2 mW of power for a 2Hz frequency. The larger than expected current draw could be a result of the foil flap of multiple valves sharing the same electrical connection. As a voltage is applied to all of the foil flaps, the flaps will induce a capacitance in the electrodes they are near even though those electrodes are not connected to the voltage source. The extra capacitance would produce a larger current draw than expected. Additionally, the valve could have been hooked to a signal generator and a more accurate root mean square could have been determined.

Conclusion

The novel valve was tested according to tests described in Chapter 3. The initial prototype built with ITO glass slides was tested only for functionality and found to be fully functional before a PCB integrated valve was constructed. The PCB valves were tested to verify functionality, operational pressure and voltage relationship, pressure and flow relationship, maximum pressure, cycles to failure and power consumption.

A digital pressure sensor was used to measure the manifold pressure. A multimeter was used to measure the voltage applied to the valve through a high voltage DC power supply. The maximum operational pressure and voltage relationship developed in Chapter 2 was validated and verified as shown in Figure 18. LABVIEW was used to record the cycles to failure test. The cycles to failure test was conducted on three valves. The three tested valves appeared to have failed for similar reasons and operated for 46378 cycles. Failure was deemed to be caused from electrical separation of the copper foil flap and the PCB traces connected to the outside voltage source. The maximum pressure the valve was able to withstand was found to be 197 kPa and was

significantly greater than the maximum operational pressure the valve was able to operate given the voltage. The power consumption was tested and resulted in a consumption of 2.2 mW, which was greater than expected.

Long-term goals for this project would include improving the PCB trace layout design to allow for the use of standard PCB solder mask as the dielectric insulator. Additionally, a more permanent electrical connection between the copper foil and the PCB traces should allow for greater cycles to failure. The double sided tape structure could be replaced with a more permanent, solid structure such as a Mylar® film. If a nonadhesive structure layer were used, then it is suggested that the valve be encased which would seal the valve and would help reduce the ballooning effects of the pressurized manifold.

CHAPTER 5

CONCLUSION AND FUTURE WORK

It was desired that a microvalve be constructed that could replace the current solenoid valves being used in a microfluidic device. Several different ideas were suggested for automatic operation of the valve, but eventually electrostatics was determined for use as the actuating force. A three-way valve was desired to allow a bladder or other container to be inflated and then deflated through the same valve. The electrostatic actuated automatic valve had to be easily assembled such that several hundred could be made within a day or two at most. The valve also had to be fairly inexpensive such that it would justify replacement of the currently proven solenoid valves.

The first working prototype of this valve was constructed with two glass slides coated with an indium tin oxide thin film. The flap was constructed of a copper foil that was 10 μm thick by 2 mm wide and 10 mm long. An insulating layer of Durimide® 284 polyimide was spun on the glass slides and inlet and outlet holes drilled into the slide. The valve and inlet path structure was created with double sided tape between the glass slides. When a voltage was applied, the foil flap would cover the outlet hole and stop the air flow. This design was the first working prototype to prove that the envisioned

electrostatic actuated microvalve fabricated in PCB could successfully stop the flow of a gas.

The design was then integrated into a PCB substrate. The PCB traces acted as electrodes and as wire traces to connect to the outside voltage source. While designing the PCB version of the valve, the size of the trace layer was neglected. This ended up to be a critical error and required inventive ways to overcome the relative rough surface caused by the copper trace undulations. The surface of the printed circuit boards was flattened with the use of adhesive transfer tape and Mylar® sheets. The flat surface was insulated with adhesive transfer tape and a thin Kapton film. The tape structure was then built such that 10 valves on one chip shared an inlet manifold. The same copper foil valve flap, proven to work with the ITO prototype, was also used for the PCB prototype. The valve was found to work with this design and was repeatable.

The PCB integrated electrostatic actuated micro gas valve was then tested to validate the theoretical performance of the valve voltage and pressure relationship. The actual relationship between valve pressure and voltage was found to have a similar trend as the theoretical prediction. The actual pressure and voltage relationship closely reflected the theoretical prediction if an increased distance between electrodes were included in the theoretical calculations. This finding allows for the conclusion that the actual valve was operating just as the theoretical model predicted, but at a larger electrode spacing than was calculated in the original model. This increased spacing is thought to have occurred due to the ballooning effect the manifold pressure had on the upper printed circuit board causing an increase in spacing between electrodes.

The PCB valve was tested to determine the number of cycles it could endure. Three valves were tested to failure. The three failed valves gave a minimum of 39,150 cycles to failure and a maximum of 46,378 cycles to failure. Failure was concluded to be caused by the copper foil flap ceasing to hold an electrical connection between the foil and the PCB trace. The failure of the valve could be due to the foil flap not being secured to the proper PCB trace through additional mean other than a press fit caused from the tape structure. If these copper foils are soldered to the tin coated traces, just as is done with a surface mount PCB component, this type of failure could be avoided.

The valve was tested to hold a maximum manifold pressure of 197 kPa before double side tape structure ruptured. Because this pressure was above the maximum operational pressure for the valve, the valve could not actuate for function at this pressure. This test was performed to determine the quality of the tape structure as a building material for a valve application.

This prototype was found to be effective an effective valve however, as a first iteration, it failed to meet many design requirements, Table 4. With future work and simple design changes, this valve could be a relatively inexpensive and reliable valve appropriate for possible single use or disposable applications.

Future Work

The valve, as designed, built, and tested, was found to be a sound design. It reacted as theoretically predicted, if an accounting is made for an increased spacing between electrodes. The prototypes built in the project show that the principles surrounding this valve could work, and work reliably for a significant amount of time.

Table 4. A comparison between the goals desired in the final production valve and the initial prototype valve results.

	Production Valve Goals	Prototype Valve Results
1	Valve density of at least 5/cm^2	0.8 valves per cm^2
2	Valve functional at 2 Hz	2 Hz functionality
3	Valve lifetime of at least 10 million cycles	A maximum of 46,000 cycles was tested
4	Valve functional to 345 kPa back pressure	17.0 kPa was the maximum valve functionality pressure
5	Valve power requirements of less than 100 mW average power	2.2 mW Measured power consumption
6	Minimum 50 valve system required	Valve chip consists of 10 valves, quick assembly allows for a 50 valve system
7	Flow rate through the valve of up to 10 l/min	215 ml/min maximum functional flow rate
8	Valves integrated into PCB to simplify electronic integration	Valve successfully integrated into PCB

Improvements to the printed circuit board would help the valve become more reliable, less expensive, more quickly assembled, and better packaged.

Neglecting of the height of the copper traces when laying out the PCB design was a critical error, and with an improved PCB lay out, problems caused by the poor trace layout could be eliminated completely. It is suggested that the improved design would incorporate the use of filled vias to carry the electrical connection to traces on another layer instead of traces on the same side of a two layer board. This would correct the

undulation problem found in the tested design, which would completely eliminate the need to flatten the PCB with adhesive and Mylar® sheet. It would also allow for solder mask to be used as the insulating dielectric instead of an adhered Kapton film, Figure 24.

Changes in the valve building material could improve the valve significantly. The current use of double sided tape was a good building material to allow cheap, accurate, layered structures, but lacked the strength to allow for large pressures. The use of double sided tape as a structural layer has draw back of possibly being unreliable. Although it was found in the research that the pressure this valve could handle was dominated by the dielectric strength of the insulation layer and the applied voltage and not the use of double sided tape as a building structure, the use of tape allows for one more failure mode that could otherwise be avoided if another building material was used. It is suggested that an improvement would be the use of some other thin membrane to accurately build the valve cavity.

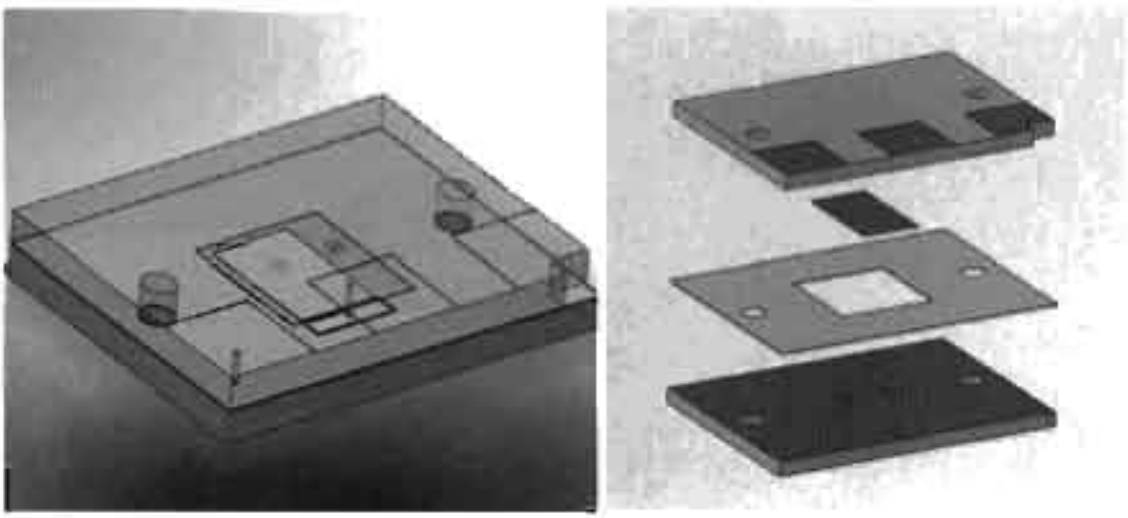

Figure 24. A proposed new PCB trace layout would eliminate the channel affected, allow solder mask to be used as the dielectric and filled vias between layers to allow built in electrical connections.

Once assembled, the valve, consisting of: a lower PCB with inlet and outlet; structure building layer; foil layer; and upper PCB with bond pads, could be incased in a packaging resin to seal it and add strength to help negate the ballooning effect of the pressurized valve cavity.

An increase to valve voltage could be used. The operational flow rate and pressure are directly related to the voltage used to actuate the valve. The validation of the valve's theoretical model shows that the manifold pressure increased in proportion to the square of the voltage. Thus, an increased voltage would have a high impact on the flow rate without an increased PCB footprint which is not typically desirable. As far as the valve is concerned, the voltage used would be limited only by the dielectric strength of the insulating layer. If the suggested improved PCB layer was used, the dielectric could be a solder mask with a dielectric strength of 110 V/micron.[24] The solder mask would be thinner than the dielectric used on the current PCB prototype and therefore an increased electrostatic force could be generated in less voltage. A careful balance exists between the thickness of the insulating layer, the voltage and the dielectric strength for optimizing the electrostatic force. A maximum voltage should be found which then can determine the thickness of the dielectric based on the dielectric strength. This should optimize a valve for maximum electrostatic force and thus maximum pressure and flow.

The electrostatic actuated micro valve has a bright future. The novelty of this valve is its electronic actuation and PCB integration. The integration of this valve into a PCB format allows for processes that are already commercially available to be applied to micro fluidics. The future of PCB integrated micro fluidics would benefit from a valve that was PCB integrated to allow for electronically controlled actuation along side the

PCB micro fluidic channels. For designs that currently use pneumatically controlled micro mixers, valves and pumps, this micro electrostatic valve could be used to automatically control the pneumatics. Use in this fashion was among the motivations to develop this microvalve and with some simple PCB layout modifications, this valve as a viable solution to many microfluid control problems can be realized.

REFERENCES

[1] Maxwell, J., 2007, "Design and Fabrication of an Actuation Module Using Integrated Pneumatic Technology." University of Utah, Salt Lake City.

[2] Hui Liu, R., Yang, J., Lenigk, F., Bonanno, J., and Grodzinski, P., 2004, "Self-Contained, Fully Integrated Biochip for Sample Preparation, Polymerase Chain Reaction Amplification, and DNA Microarray Detection." Analytical Chemitry, **76**, pp. 1824-1831.

[3] Eddings, M., 2006, "A Review of Pneumatically-Actuated Micropumps and Microvalves." Microfluidic Design, **1**(2), pp. 1-12.

[4] Feng,G., and Kim, E., 2004, "Micropump Based on PZT Unimorph and One-Way Parylene Valves." J. Micromech. Microeng., **14**, pp. 429-435.

[5] Sershen, S., Mensing, G., Ng, M., Halas, N., Beebe, D., West, J., 2005, "Independent Optical Control of Microfluidic Valves Formed from Optomechanically Responsive Nanocomposite Hydrogels." Advanced Materials, **17**, pp. 1366-1368.

[6] Ho, T., 2007, "Preliminary Design, Manufacture and Characterization of a Novel Paraffin-Based Microactuator for Microfluidic Devices." University of Utah, Salt Lake City.

[7] Yang, B., Lin, Q., 2006, "A Latchable Microvalve Using Phase Change of Paraffin Wax." Sensors and Actuators A, **134**(1), pp. 194-200.

[8] Fu, C., Rummler, Z., Schomburg, W., 2003, "Magnetically Driven Microball Valves Fabricated by Multilayer Adhesive Film Bonding." J. Micromech. Microeng., **13**, pp. S96-S102.

[9] Tomonari, S., Yoshida, H., Kamakura, M., Yoshida, K., Kawahito, K., Saitoh, M., Kawada, H., Juodkazis, S., Misawa, H., 2003, "Efficient Microvalve Driven by a Si-Ni Bimorph." Jpn. J. Appl. Phys., **42**, pp. 4593-4597.

[10] Grover, W., Ivester, R., Jensen, E., Mathies R., 2006, "Development and Multiplexed Control of Latchin Pneumatic Valves Using Microfluidic Logical Structures." J. of The Royal Society of Chemistry, **6**, pp. 623-631.

[11] Grosjean, C., Yang, X., Tai, Y., 2002, "A Thermopneumatic Microfluidic System." *The 15th IEEE International Conference on Micro Electro Mechanical Systems*, IEEE., Las Vegas, pp. 24-27.

[12] RAZOR® EX System. Idaho Technology, Inc. www.idahotech.com

[13] Takagi, S., Sasaki, H., Shikida, M., Sato K., 2007, "Electrostatic Latch Mechanism for Handling Projection on Arrayed Vertical Motion System." *14th International Conf. on Solid-State Sensors, Actuators and Microsystems*, IEEE, Lyon, pp. 1147-50.

[14] Messner, S., Schaible, J., Vollmer, J., Sandmaier, H., Zengerle, R., 2006, "Electrostatic Driven 3-way Silicon Microvalve for Pneumatic Applications." Microfluidics and Nanofluidics, **2**(2), pp. 89-96.

[15] Gale, B., 2007, University of Utah Dept. of Mech. Engineering, Salt Lake City.

[16] Saucedo-Flores, E., Ruelas, R., Flores, M., Chiao, J., 2003, "Study of the Pull-In Voltage for MEMS Parallel Plate Capacitor Actuators." A5.86, *Matateriał Research Society Symposium Proc.*, LaVan, D. et al., eds., Material Research Society, Warrendale, **782**, pp. 1-7.

[17] Technical Data Sheet, 2006, "3M Adhesive Transfers Tapes with Adhesive 300" 3M, St. Paul.

[18] Technical Data Sheet, 2006, "DuPont™ Kapton® HN" DuPont High Performance Materials, Circleville.

[19] Budynas, R. G., Nisbett, J. K., 2008, *Shigley's Mechanical Engineering Design*, 8th Edition, McGraw-Hill, Singapore, pp. 278-289, Chap. 6.

[20] Technical Data Sheet, 2009, "Metal-Mechanical Properties" Goodfellow Corporation, Oakdale.

[21] SMC S070, SMC Corportation of America, http://www.smcusa.com.

[22] O'Malley, M., McStravick, D. M., 2008, Mech 401 Mechanical Design Applications Lecture Slides, Rice University.

[23] ASTM Standard F1373-93, 2005, "Standard Test Method for Determination of Cycle Life of Automatic Valves for Gas Distribution System Components," ASTM International, West Conshohocken, PA, DOI: 10.1520/F1373-93R05.

[24] Technical Data Sheet, 2002, "Final Properties for PSR-4000HG (DG)" Taiyo Ink Mfg. Co., Ltd., Carson City.